Mechanisms of multi-particle production processes

I. V. Andreev and I. M. Dremin

P. N. Lebedev Physics Institute, USSR Academy of Sciences
Usp. Fiz. Nauk **122**, 37–79 (May 1977)

PACS numbers: 12.40.Bb, 12.40.Ee, 12.40.Mm, 12.40.Ss

CONTENTS

1. INTRODUCTION

Particle-particle interactions at high energy lead in most cases (~80%) to the production of new particles. The number of newly produced particles rises as a function of the collision energy. Thus multi-particle production becomes the dominant process at sufficiently high energies.

It is quite clear that the character of this process is directly determined by the internal structure of the particles. Consequently, there can be no genuine understanding of particle structure without an understanding of multiparticle production. However, we cannot say that we are close to such an understanding at the present time. So far, no unified or systematic model has been constructed for the description of multiparticle production processes; instead, there are several different approaches intended to describe certain aspects of the experimental data. Owing to the diversity of such approaches, we are obliged to begin with a preliminary, though perhaps highly provisional, classification of these approaches.

There is a large group of models based on the idea that two colliding hadrons form a single excited system. This class of models includes the hydrodynamic and statistical (thermodynamic) models and the statistical bootstrap.

It is sometimes assumed that the process of particle production takes place through the excitation and subsequent decay of each of the colliding particles, i.e., that two systems are produced, reflecting to some extent the individuality of the primary hadrons. This group of models includes the fragmentation model, the bremsstrahlung model, and the model of inelastic diffraction.

The largest and perhaps most successful group of models describes multiparticle production processes as a result of the production of many excited subsystems. The most typical representative of this class is the multiperipheral model, which is closely related to the inclusive Regge approach, the parton description of multiparticle production processes, and the model of independent emission of clusters and uncorrelated jets. The eikonal approximation is often used to take into account multiple interactions.

An interesting approach is represented by direct attempts to relate the mechanisms of multiparticle production processes to the internal structure of the particles—their constituents, quarks, gluons, etc.

In addition to such models, there have been attempts to find phenomenological relations among the various characteristics of multi-particle production processes.

Of course, the foregoing classification is a matter of convention, since models within a single group may differ from one another with regard to their assumptions and conclusions and, conversely, models from different groups may have similarities. For example, models of the statistical-thermodynamic type are often used to describe the decays of independently emitted clusters. The parton model with multiperipheral spectra is closely related to quark models.

The domains of applicability of the models are determined by the experimental facts regarding the existence of leading particles (which have high energy in the center-of-mass system) and pionization particles (which are slow in the c.m.s.).

Fragmentation models can be applied to the leading particles (as well as to quasi-two-body reactions). These particles are produced in the multiperipheral picture from the extreme rungs of the diagram or in constituent models as penetrating groups of quarks.

At the same time, statistical ideas can be applied to

the residual pionization particles (either to all of them collectively or to subsystems of these particles produced as a result of a multiperipheral process or some other mechanism). Models for describing multi-particle production processes therefore usually have a multicomponent character.

Each of the approaches mentioned above has been reflected to some extent in books, conference proceedings, and review papers (see, e.g., Refs. 1–5). As a supplement to such reviews, it would be useful to compare the principal results of these models with one another and with the experimental data (see, in particular, Refs. 1 and 2), without excessive elaboration of the theoretical calculations, and to discuss once again the proposed modifications of the models and the manner in which they have been developed. These are our aims in writing the present review, which is based on a rapporteur's report presented by one of the authors (I.D.) at the Conference on High Energy Physics.

As we have already mentioned, the experimental data provide an important criterion for selecting the domains of applicability of models and specifying their free parameters. We therefore begin by recalling briefly (as far as possible within the scope of this review) the main experimental facts about inelastic interactions of hadrons at high energies. We shall then discuss the basic hypotheses of the most popular models of multiparticle production and compare their predictions with the experimental data. As the interactions of hadrons with nuclei have a rather specific character, they are discussed in a separate section. An analysis of the space-time region of the hadron-hadron interaction also provides certain information about the mechanisms of multiparticle production. Finally, we shall consider briefly what results might be expected from the new generation of proton accelerators at super-high energies.

2. A BRIEF REVIEW OF THE EXPERIMENTAL DATA AT ACCELERATOR ENERGIES

A. The total cross sections

The total cross sections for strongly interacting particles amount to tens of millibarns ($\sim 10^{-26}$ cm^2); this implies that the effective range of the strong interactions is of the order of 1 F.

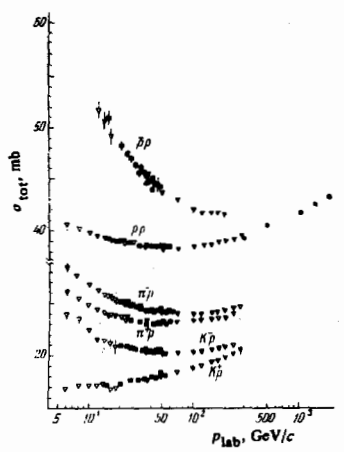

FIG. 1. The energy dependence of the total cross sections for hadron–hadron interactions.

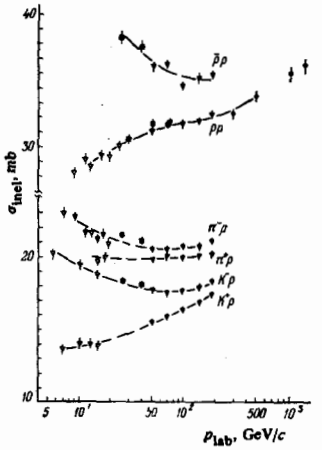

FIG. 2. The energy dependence of the cross sections for inelastic interactions.

The total cross section for the proton-proton interaction has been measured over the largest range of energies (up to $p_{lab} \approx 2000$ GeV/c). The fall-off in the total cross section (Fig. 1) up to the energies of about 30 GeV gives way to a broad minimum in the range of energies from 30 to 70 GeV and a slow growth at higher energies (by ~12% at $p_{lab} \approx 1500$ GeV/c). The total cross sections for the interactions of pions, kaons, and antiprotons with protons, which have been measured up to 280 GeV, exhibit similar trends, although they differ from one another in their low-energy behavior and in the positions of their minima (see Fig. 1). The high-energy growth is more conspicuous in the behavior of the cross sections for inelastic interactions (Fig. 2).

B. The multiplicity of secondary particles

The average number of secondary particles produced in high-energy collisions arises with increasing energy. However, this growth is much weaker than the maximally possible growth ($\sim E_{cm}$).

Various phenomenological approximation formulas have been proposed[6] to describe this growth. The accelerator data, supplemented by data obtained from cosmic rays, seem to be best described (Fig. 3) for energies $\sqrt{s}$ in the range from 3 to 150 GeV by formulas

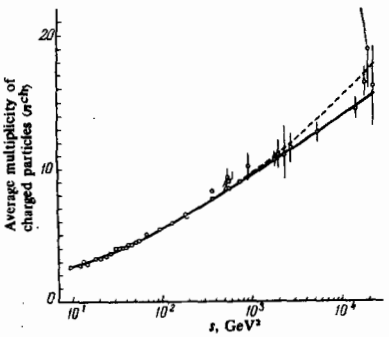

FIG. 3. The energy dependence of the average multiplicity of charged particles in pp interactions. The solid curve corresponds to the expression $1.99 \ln s + 8.16 s^{-1/2} - 4.55$, and the dashed curve corresponds to $0.13 \ln^2 s + 0.30 \ln s + 1.17$.

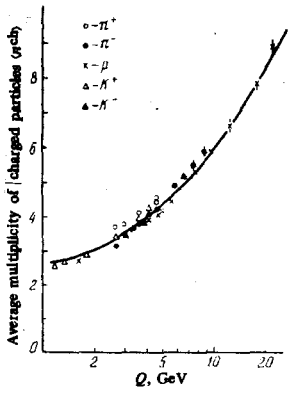

FIG. 4. The average multiplicity of charged particles in π^+p, K^+p, and pp interactions as a function of the available energy $Q=\sqrt{s}-m_a-m_b$. The curve has the same significance as in Fig. 3 (the difference between the solid and dashed curves is negligible here).

of the type

$$\langle n^{\mathrm{ch}}\rangle = A + B\ln s + C(\ln s)^2. \tag{2.1}$$

However, if we confine ourselves to energies $\sqrt{s}$ above 10 GeV, a sufficiently good fit is obtained with a logarithmic dependence

$$\langle n^{\mathrm{ch}}\rangle = a_0 \ln s + b_0. \tag{2.2}$$

where $a_0 \approx 1.5$–2 and $b_0 \approx (-1)$–(-2), or with a formula of the type

$$\langle n^{\mathrm{ch}}\rangle = cs^d, \tag{2.3}$$

where $d \approx 0.2$.

It is interesting to observe that for the most diverse types of colliding particles a and b the average multiplicity of secondary charged particles at high energies is a universal function of the energy release of the reaction defined by $Q=\sqrt{s}-m_a-m_b$ (this has been verified for $a=p$, $\pi^\pm$, $K^\pm$, γ, μ^+, e^-, ν, $\bar{\nu}$ with $b=p$ and for $a=e^+$ with $b=e^-$; see Fig. 4), i.e., this multiplicity is independent of the type of incident particle or target particle.

The higher moments of the multiplicity distribution also rise with energy. The distributions themselves conform quite well to the requirement known as KNO scaling, i.e., the topological cross sections for producing n particles (σ_n) depend only on the ratio $n/\langle n\rangle$:

$$\frac{\sigma_n}{\sigma_{\mathrm{inel}}} \sim \frac{1}{\langle n\rangle}\Psi\left(\frac{n}{\langle n\rangle}\right), \tag{2.4}$$

where the function Ψ is universal for all hadronic reactions (Fig. 5). This implies, in particular, that the dispersion D of the distribution has exactly the same energy dependence as the average multiplicity $\langle n\rangle$.

C. Longitudinal momentum distributions

Although the initial particles have large momenta in the center-of-mass system, the secondary particles are produced with relatively small momenta. Most of the secondary particles are produced in the so-called pionization region, which is conventionally restricted by the inequality

$$x=\frac{2p_L}{\sqrt{s}}<0.1 \tag{2.5}$$

(where p_L is the longitudinal component of momentum of a secondary particle in the c.m.s.).

Some of the particles are produced as a result of fragmentation of the colliding hadrons:

$$0.1 \leqslant x \leqslant 0.8\text{–}0.9, \tag{2.6}$$

and the non-excited recoil nucleons in inelastic diffraction fall in the range

$$0.9 \leqslant x \leqslant 1. \tag{2.7}$$

Another variable which is widely used is the rapidity y:

$$y=\frac{1}{2}\ln\frac{E+p_L}{E-p_L}. \tag{2.8}$$

In the rapidity variable, the pionization region occupies the major portion of the admissible interval of y, which grows with energy, while the fragmentation and diffraction regions may occupy the edge of this interval, with a finite width as $s\to\infty$.

The energy dependence of the invariant cross sections in the pionization region is naturally of special interest. According to the concept of Feynman scaling, the invariant cross sections at high energies should depend only on x and on the transverse momentum component p_T, and not on the energy:

$$\lim_{s\to\infty} E\frac{d^3\sigma}{d^3p} = F(x, p_T). \tag{2.9}$$

In view of the observed growth of the total cross sections, the condition (2.9) can be replaced by the requirement

$$\lim_{s\to\infty} \frac{E}{\sigma}\frac{d^3\sigma}{d^3p} = f(x, p_T). \tag{2.10}$$

Neither of the conditions (2.9) or (2.10) is satisfied experimentally over the entire range of values of x at

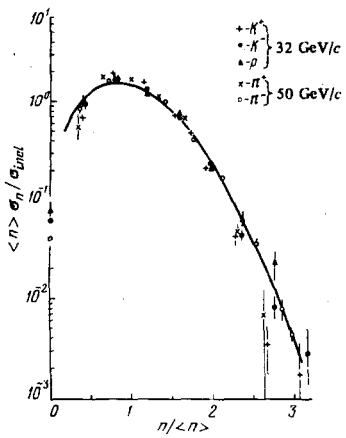

FIG. 5. The distributions in the number of charged particles. The curve for the pp interaction is for a wide range of energies (from 50 to 303 GeV) ($\blacktriangle-\bar{p}$).

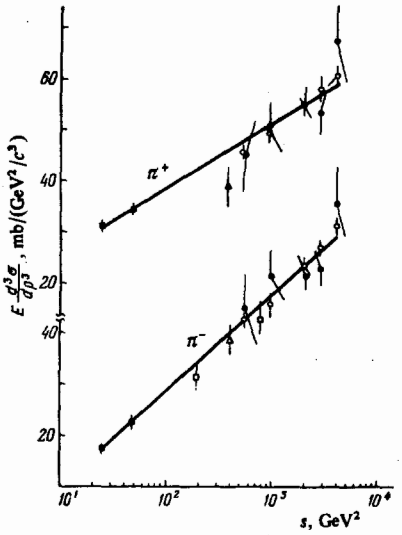

FIG. 6. The growth of the inclusive cross section in the pionization region ($x = 0$) as a function of energy. The solid curves correspond to the approximation formula $A + B \ln s$.

currently accessible energies (up to $\sqrt{s} = 63$ GeV). It is true, however, that the condition (2.10) is quite well satisfied in the fragmentation region above $\sqrt{s} = 8$ GeV. This phenomenon is known as "early scaling." However, the invariant cross section for charged-pion production in the pionization region (at $x = 0$) rises[7] by a factor 1.5–2 over the range of $\sqrt{s}$ from 5 to 23 GeV (Fig. 6) and by approximately a further 40% as $\sqrt{s}$ varies over the ISR energy range from 23 to 63 GeV (alternatively, eliminating the growth of the total cross sections in this range according to (10), we obtain a 25% growth of the quantity $(E/\sigma)d^3\sigma/d^3p|_{x=0}$[1)]).

The distributions in y at a given energy are bell-shaped, with a depression at the top (Fig. 7). But there is no strictly constant plateau even in the pionization region, and the cross sections fall off by about 10–15% as the rapidity in the c.m.s. varies from 0 to 1.[8] The absence of an "asymptotic" central plateau is most apparent in reactions involving non-identical initial particles (such as πp interactions), in which case the distribution in y exhibits a conspicuous asymmetry, i.e., it "remembers" the directions of motion of the incident proton and pion.

D. Transverse momentum distributions

Most of the secondary particles are produced with small transverse momenta (the average value is $\langle p_T \rangle \approx 0.35$ GeV/c). The differential cross section for pion production falls off exponentially (Fig. 8) as a function of the transverse momentum up to values $p_T \sim 1.5$–2.0 GeV/c over the entire accessible range of high energies according to the law

$$E\frac{d^3\sigma}{d^3p} \sim \exp(-6p_T) \qquad (2.11)$$

(here p_T is expressed in GeV/c).

[1)]The cross sections for producing the heavier particles K and $\bar{p}$ grow even more rapidly in this energy range.

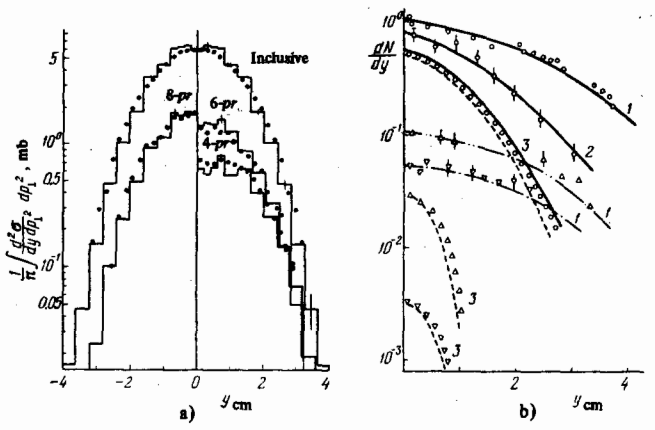

FIG. 7. The inclusive rapidity distribution of pions produced in pp collisions. (a) The experimental data at 69 GeV are shown as histograms for 4-, 6-, and 8-prong events and for the sum of all events. The points show the results calculated according to the multiperipheral model.[121–123] (b) The inclusive distributions for $\pi^-(0)$, $K^-(\Delta)$, and $\bar{p}(\nabla)$ at $s = 2800$ GeV^2 (curve 1), 388 GeV^2 (curve 2), and 46.8 GeV^2 (curve 3); the curves are the fits of the hydrodynamic theory (for details of the calculations, see Ref. 38).

A strong deviation from the exponential law (2.11) is observed for large values $p_T > 2.0$ GeV/c, where the fall-off becomes slower. The results obtained in this region of transverse momenta are very extensive, and their interpretations differ somewhat from the principal mechanisms of multiparticle production which are used for small transverse momenta. Therefore we shall not consider these data here (we shall only occasionally mention them when they have an obvious bearing on one of the mechanisms of multiparticle production which we discuss).

E. Correlations

Single-particle inclusive distributions provide only average information about multi-particle production processes. More detailed information can be obtained by studying the correlations between the secondary particles. However, this involves two major problems. First, it is desirable to know not only the correlations between two particles, but also multiparticle correlations; second, these data should be visualizable, i.e., it is necessary to select the most important variables

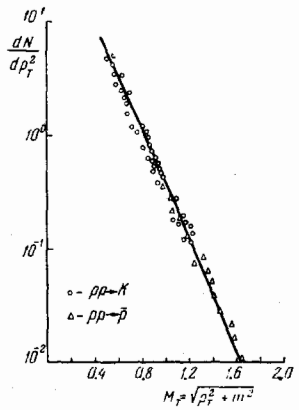

FIG. 8. The pion distribution with respect to the transverse momentum. The solid curve is the fit to the data by statistical formulas (for details of the calculations, see Ref. 38). This curve practically coincides with the data on $pp \to \pi^+ X$ at ISR energies. The triangles are the data on $\bar{p}$ production, and the circles are the data for kaons.

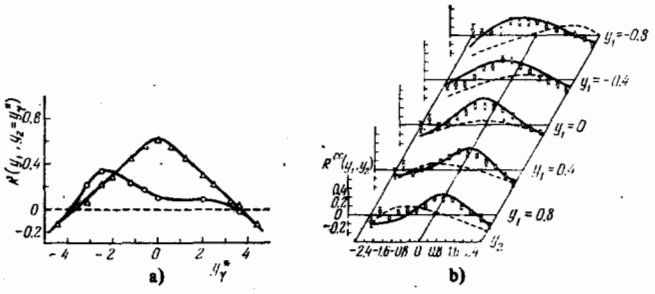

FIG. 9. (a) The correlation of charged pions and neutral pions (photons from their decays) at $\sqrt{s}=30$ GeV (the values of the function $R(y_1, y_2=y_\gamma^*)$ for a charged-pion rapidity $y_1=0$ or $y_1=-2.5$ are indicated by the triangles and circles, respectively); (b) the correlations of charged pions in the reaction $\pi^- p \to \pi\pi + X$ at 40 GeV (the points are the experimental data, the dashed curves are the phase-space calculations, and the solid curves are calculated according to the multiperipheral model[121–123]).

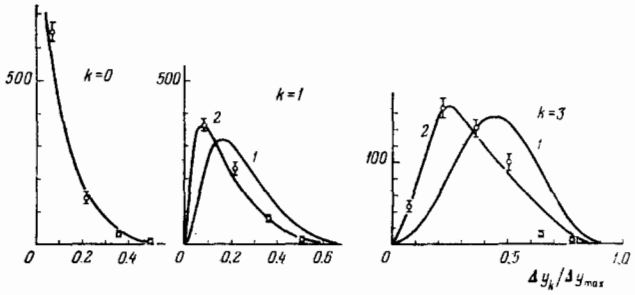

FIG. 11. The distributions of rapidity intervals at 200 GeV. The number of particles inside the interval is denoted by k. The 8-prong events have been selected ($n^{ch}=8$). The curves labeled 1 and 2 correspond to independent particle emission and cluster emission, respectively.

from the entire set of possible variables. In fact, even a two-particle system is described by the six components of the particle momenta, the masses, charges, etc. As the number of particles increases, the problem of correctly choosing the variables becomes more and more complicated. It is now most popular to study the correlations between the longitudinal momentum components (or rapidities) of the secondary particles.

In particular, the two-particle correlations are studied by comparing the distributions with respect to the rapidities (y_1 and y_2) of the two particles, $\partial^2\sigma/\partial y_1 \partial y_2$, with the product of the single-particle distributions, $(\partial\sigma/\partial y_1)\partial\sigma/\partial y_2$. Use is also made of the functions

$$C(y_1, y_2) = \frac{1}{\sigma_{\text{inel}}} \frac{\partial^2\sigma}{\partial y_1 \partial y_2} - \frac{1}{\sigma_{\text{inel}}^2} \frac{\partial\sigma}{\partial y_1} \frac{\partial\sigma}{\partial y_2} \tag{2.12}$$

and

$$R(y_1, y_2) = \frac{\sigma_{\text{inel}} \partial^2\sigma}{(\partial\sigma/\partial y_1)\partial\sigma/\partial y_2} - 1. \tag{2.13}$$

The experimental data (Fig. 9) show that there are appreciable correlations between particles with similar rapidities (so-called short-range correlations); these correlations show up in the form of the maximum of the function $R(y_1, y_2)$ for $y_1=y_2$. Long-range correlations between particles show up in variations in the form of the correlation functions for variations in the position of the maximum (compare the curves in Fig, 9 for $y_1=0$ and $y_1=2.5$). In addition to the inclusive correlation functions (2.12) and (2.13), studies are also made of the semi-inclusive correlation functions C_n and R_n when the number of particles n is specified.

If each event is accompanied by information about the rapidities of all the (usually charged) particles, it is possible[9] to study the two-particle correlations by means of the distribution in the nearest-neighbor spacings ("gaps") in the rapidity variable. These distributions have a sharp peak at small spacings for energies between 100 and 400 GeV (Fig. 10).

This approach can easily be generalized to multiparticle correlations[10] by studying not only the distribution of vacant rapidity intervals, but also the distributions of intervals containing $1, 2, 3, \ldots, k \leq n-2$ particles.[2)] Such distributions at 200 GeV are shown in Fig. 11.

All these methods are usually used in the analysis of particle clusterization effects (see Sec. 7C). In addition to analyses of rapidity correlations, studies are often made of the correlations of the particles in their azimuthal and pair masses, and of the properties of local compensation of transverse momenta, charge, etc. The conclusions obtained by analyzing these characteristics of the process are discussed later.

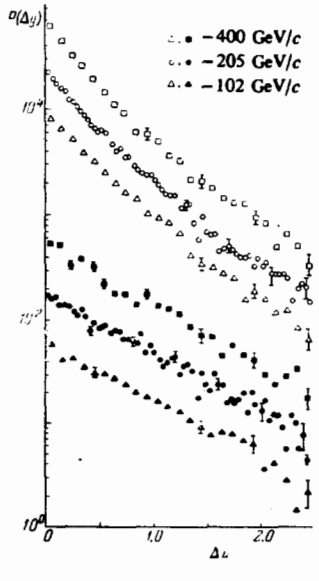

FIG. 10. The distributions of rapidity gaps at energies between 100 and 400 GeV. The light points are for all charged particles, and the heavy points are for negatively charged particles.

F. Hadron–nuclear interactions

Hadron–nuclear interaction cross sections have the approximate dependence $A^{2/3}$, where A is the number of nucleons in the nucleus. This means that the nucleus represents a highly opaque object for the hadrons. The experimental data[11] can be parametrized by the expressions

[2)] We note that the generalization of the method of C and R functions is much more complicated, since it requires an analysis of multi-dimensional distributions.

$$\sigma_{\pi A} = 28.5\, A^{0.75}\ \text{mb}, \quad \sigma_{pA} = 46\, A^{0.69}\ \text{mb}. \tag{2.14}$$

Most of the experimental data on the multiplicities refer to emulsions. The particles detected here are fast charged particles (n_s; $\beta = v/c > 0.7$) and "heavy particles" (N_h; $\beta < 0.7$). The average multiplicity $\langle n_s \rangle_A$ in relation to the multiplicity $\langle n_s \rangle_p$ on the nucleon has only a weak dependence on the atomic number A. Using a power-law parametrization

$$R_A = \frac{\langle n_s \rangle_A}{\langle n_s \rangle_p} \sim A^{\alpha} \tag{2.15}$$

the emulsion data yield a value $\alpha \sim 0.12$–0.15. The data are compatible with a value of R_A which is independent of the energy E from $E \sim 60$ GeV up to $E \sim 10^4$ GeV (where $R_A \approx 1.8$). The multiplicity distribution satisfied KNO scaling, and the function $\Psi(n/\langle n \rangle)$ (see Eq. (2.4)) is similar to the corresponding hadron–hadron function.

The data on inclusive distributions indicate that the growth of the multiplicity, i.e., the deviation of R_A from the unity, is due to the production of particles at large angles. Accordingly, the inclusive quantity

$$R_A(y) = \frac{(1/\sigma_{hA})\,(\partial\sigma/\partial y)_{hA}}{(1/\sigma_{hN})\,(\partial\sigma/\partial y)_{hN}} \tag{2.16}$$

is appreciably greater than unity in the fragmentation region of the nucleus and is less than (or close to) unity in the fragmentation region of the incident particle.

Data which refer specifically to hadron-nuclear interactions and which characterize the response of the nucleus are of special interest. The number of produced particles is large, $N_h \sim A^{2/3}$, and is independent of energy; this suggests a process which increases the number of slow particles and the rapid onset of the regime of limiting fragmentation of the nucleus. In the momentum region which is kinematically forbidden for hadron–hadron interactions (the emission of "backward" particles), the inclusive distribution $(1/\sigma_{\text{tot}})Ed^3\sigma/d^3p$ is independent of both the type of incident particle and the initial energy above 10 GeV. The number of fast particles as a function of the energy and of the number of heavy particles also factorizes:

$$\langle n_s(N_h, E) \rangle = \langle n_s \rangle_p F(N_h). \tag{2.17}$$

3. THE STATISTICAL-HYDRODYNAMIC APPROACH

The experimental data on inclusive spectra at high energies have recently led to renewed interest in statistical-hydrodynamic models. This is largely due to the form of the rapidity distributions of the particles, which is unlike a flat "plateau," and to the energy dependence of these distributions, which is inconsistent with the idea of scaling (see Sec. 3C). Moreover, only such models can provide a natural explanation of the exponential suppression of the transverse momenta of the produced particles (see Sec. 2D). The physical content of these models is also attractive[3)].

As is well known, the statistical approach to the problem of multi-particle production is based on the assumption, first proposed and developed in the 1950s,[13,14] that the single system (or subsystem) produced in a hadron–hadron collision quickly comes into a state of thermodynamic equilibrium because of the great strength of the hadronic interactions. Three stages can be distinguished in this process:

1. An initial stage, involving randomization and production of a highly excited system.

2. A hydrodynamic and isoentropic expansion.

3. A final stage, in which the system decays into real secondary particles.

To give a complete description of the evolution of this system, it is necessary to specify the following details:

a) the laws of energy-momentum conservation;
b) the statistical momentum distribution of the particles;
c) the equation of state;
d) the chemical potential;
e) the initial conditions and decay conditions of the system;

As an example, which can be meaningfully compared with all subsequent modifications of the theory, we give an outline of Landau's hydrodynamic theory.[15] The law of energy-momentum conservation is written in the form

$$\frac{\partial T_{ik}}{\partial x_k} = 0. \tag{3.1}$$

where

$$T_{ik} = (\varepsilon + p)\, u_i u_k - p g_{ik} \tag{3.2}$$

is the energy-momentum tensor of an ideal relativistic fluid, ε is the energy density, p is the pressure, u_i are the components of the 4-velocity vector of the fluid, and g_{ik} is the metric tensor ($g_{00} = -g_{ii} = 1$).

The pion distribution with respect to the momentum q in the proper system of a volume element at the instant of decay is given by the usual Bose statistical distribution:

$$dN = \frac{gV}{(2\pi)^3} \frac{d^3q}{e^{E/T} - 1}. \tag{3.3}$$

Here $E = \sqrt{q^2 + m^2}$ is the energy of a particle, g is the number of its spin and charge states ($g = 3$ for pions), T is the temperature, and V is the final volume.

The equation of state is taken in the form

$$p = \frac{\varepsilon}{3}, \tag{3.4}$$

which holds for a three-dimensional volume filled with a gas of relativistic particles.

[3)] It is true that one can criticize the very foundations of the hydrodynamic approach, since it leads to inconsistencies with the uncertainty relations.[12] However, the interest in this approach is enhanced by the possibility of applying it to subsystems of particles and by its purely phenomenological success.

The chemical potential of the pion system is

$$\mu = 0. \tag{3.5}$$

It is therefore assumed that the number of particles is not fixed, but that it is determined by the equilibrium condition (as in the case of black-body radiation), i.e., by the condition that the thermodynamic potential is equal to zero:

$$\varepsilon - Ts + p = 0 \tag{3.6}$$

(where s is the entropy density), from which we can readily obtain the equation $\varepsilon = \varkappa T^4$.

It is assumed that at the initial instant the hadronic system takes the form of a thin disk of thickness $\sim (1/m_\pi)\, m/E_0$ (where m_π and m are the pion and nucleon masses, and E_0 is the initial energy in the c.m.s.) and radius $\sim m_\pi^{-1}$, at rest in the c.m.s. ($v = 0$ at $t = 0$). The expansion of the system takes place in accordance with Eqs. (3.1)–(3.5), and it decays into particles when the temperature of a volume element becomes of order m_π.

The physical implications of this model are well known. The main conclusions are as follows:

1) the average multiplicity rises with energy according to the law $\langle n \rangle \sim \sqrt{E_0}$;

2) the rapidity spectrum of the particles has a roughly Gaussian form, with a width that grows like $\sqrt{\ln s}$;

3) in the central region the spectrum rises with energy (i.e., there is no scaling), whereas for finite values of x there may be a very weak fall-off in the spectrum;

4) the average transverse momentum rises weakly with energy according to the law $\langle p_T \rangle \sim s^\beta$, where the value of β varies between 1/12 and 1/14 according to various estimates.

The following main trends can be distinguished in the subsequent development of the statistical-hydrodynamic approach:

a) attempts to give a more detailed description, which are reminiscent of the kinetic approach and which involve non-linear Lagrangians of field theory;

b) the introduction of a microscopic picture which takes into account the internal structure of the colliding particles;

c) revision of the equation of state and the conditions of production and decay of the system;

d) detailed comparisons with experimental data.

Attempts to introduce a more general kinetic approach from which it might be possible to derive the hydrodynamic description[16,17] are based on the use of Wigner's distribution function

$$F(p, R) = \int d^4 r e^{ipr} \left\langle \psi_{\text{in}} \left| \varphi\left(R - \frac{r}{2}\right) \varphi\left(R + \frac{r}{2}\right) \right| \psi_{\text{in}} \right\rangle, \tag{3.7}$$

where φ are operator wave functions of a field, the metric is chosen in the form (+, −, −, −), the entire analysis is made in the Heisenberg representation, and the average is taken over the "in"-states. If ψ_{in} is a two-particle state, it is easy to show, by making use of the relation between inclusive spectra and multi-particle amplitudes, that the Fourier transform of Wigner's function with respect to the variable R ($F(p, q)$) is uniquely related to the inclusive distribution of the particles with respect to the momentum p by the equation

$$2\omega \frac{d^3N}{d^3p} = \frac{(p^2 - \mu^2)^2}{(2\pi)^3} F(p,\ q = 0). \tag{3.8}$$

At the same time, one can also make use of the equations of field theory to obtain kinetic-type equations for F, whose nonlinearity is determined by the interaction Lagrangian. It is also possible[17] to exhibit a transition to the hydrodynamic theory in a certain approximation. The relation between non-linear Lagrangians of field theory and the parameters of the hydrodynamic theory was previously considered by Milekhin.[18] It is now proposed to establish this relation in the framework of the kinetic approach, in which one also considers the correspondence with the inclusive description of these processes in the Regge scheme.

The main fundamental difficulty in deriving the equation is, of course, the fact that we have no sufficiently realistic candidate for the strong-interaction Lagrangian at the present time, although the success of non-Abelian gauge theories does raise some hopes. In addition, as discussed below, the opposite situation can occur: experiment can help us to select the correct form of the strong-interaction Lagrangian.

The hydrodynamic theory usually provides only a macroscopic description of the process of expansion of the system, since it is assumed that the density of matter is larger in this case and that the interaction is so strong that the concept of a particle inside such a system becomes meaningless. Adopting the hypothesis that there are point-like constituents (partons) inside a hadron, one may propose[19,20] a new treatment of the hydrodynamics which takes into account the microscopic structure of the hadronic cluster by assuming that the statistical behavior of the constituents (and not the dynamics of their interaction) is responsible for the simplest characteristic features of the process (such as the single-particle spectrum).

In the case of conservation of the number of massive partons,[19] the properties of the system are appreciably different from Landau's hydrodynamics. In the first place, the partons obey Fermi statistics. The problem of their transformation into pions remains open. Secondly, the chemical potential is large (this guarantees the conservation of the number of partons during the expansion of the system). Thirdly, the equation of state has the form $p = \varepsilon$, which leads to $\varepsilon = \lambda T^2$ and $c_0^2 = 1$ (where c_0 is the velocity of sound). The popularity of the idea of Feynman scaling, which occurs when $c_0 = 1$, has stimulated interest in this equation of state.[17,20]

Conservation of the number of partons can also be achieved without such cardinal modifications by assuming[20] that the parton mass is equal to zero. One can then derive the same conclusions as in Landau's hydro-

dynamics by introducing some additional mechanism such as a phase transition, which ensures that the partons are transformed into hadrons. A similar picture involving a phase transition also occurs in attempts to apply the results of field-theoretic models with broken symmetry to high-energy physics[21]; in this case, the parton mass depends on the temperature.

The occurrence of a phase transition is characteristic of the statistical picture in which the thermodynamic properties of the system are expressed in terms of the scattering matrix of the particles that form this system.[22,23] The equation of state in this case is different from (3.4), and at high temperatures it takes the form $p=\varepsilon/5$.

We note that phenomenological attempts to revise the equation of state have been made previously.[16,24-27] In particular, many studies have been made of an equation of state having the form

$$p=c_0^2\varepsilon \tag{3.9}$$

for arbitrary but constant c_0. The simplest models have been used to relate the quantity c_0 to the degree of nonlinearity of the interaction Lagrangian[18]:

$$c_0^2=\frac{1}{2n-1}, \tag{3.10}$$

for

$$L_{\text{int}}=\lambda\left(\frac{\partial\varphi}{\partial x_k}\right)^{2n}. \tag{3.11}$$

This gives

$$p\sim T^{(c_0^2+1)/c_0^2},\quad s\sim T^{1/c_0^2},\quad \langle n\rangle\sim E_0^{(1-c_0^2)/(1+c_0^2)}.$$

Direct calculations have been made[25,26] of the value of c_0 as a function of the temperature, with allowance for the known resonances. Use was made of the equations

$$c_0^2=\frac{\partial p}{\partial\varepsilon},\quad p=\frac{1}{3}\sum_i\int\frac{q^2}{E_i}\left(e^{E_i/T}-1\right)^{-1}\frac{g_i d^3qV}{(2\pi)^3}, \tag{3.12}$$

$$\varepsilon=\sum_i\int E_i\left(e^{E_i/T}-1\right)^{-1}\frac{g_i d^3qV}{(2\pi)^3}, \tag{3.13}$$

where the summation was taken over the resonances. The results are shown in Fig. 12.

It can be seen that c_0^2 is close to 1/5 at high temperatures. Moreover, the best agreement with the experimental data is found for this value of c_0^2.[25,26]

We note that, according to Eqs. (3.10) and (3.11), the value $c_0^2=1/3$ corresponds to a non-linear interaction Lagrangian of the form $\lambda(\partial\varphi/\partial x_k)^4$, while the value $c_0^2=1.5$ leads to an interaction of the form $\lambda(\partial\varphi/\partial x_k)^6$. In renormalizable theories with broken symmetry, it is possible[21] to have a situation in which the law $c_0^2=1/3$ holds only at high temperatures (above a certain critical temperature), while the value of c_0^2 changes at low temperatures (owing to a phase transition at $T=T_c$).

Thus we see that the determination of the equation of

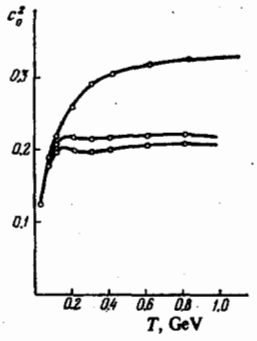

FIG. 12. The value of c_0^2, calculated by the Bethe-Ulenbeck method (see Refs. 25 and 26), as a function of the temperature T. The upper curve is obtained when allowance is made for only resonances with small masses.

state is one of the most important problems in the hydrodynamic approach, and this problem must be regarded as one which is still open. Of equal importance is the problem of choosing the correct initial conditions (for example, the presence of collective velocities at the initial instant of time may simulate the effects of a different equation of state).

Later we shall consider the quantitative comparisons with the experimental data which have been made by many authors[25,26,28-42]; here we stress that special care must always be exercised in making such comparisons to distinguish the system (or subsystem) of particles that is treated statistically.[35] This is so largely because of the peripheral character of the collisions exhibited by the energetically distinguished (leading) particles, whose treatment is clearly ambiguous in the statistical approach (cf. Refs. 24 and 25).

At the same time, this peripheral character of the collisions is the basis of fragmentation and multiperipheral models.

4. FRAGMENTATION MODELS

According to the fragmentation model,[43-46] an inelastic interaction of two hadrons leads to a transition of one or both of the hadrons into certain excited states, which then decay, generally into many particles. Only energy and angular momentum can be transferred during the interaction. All other quantum numbers of the excited system coincide with the characteristics of its parent hadron.

The production of two centers of particle emission, each of which retains a memory of its initial hadron, is a characteristic feature of the fragmentation model.[4)]

In concrete realizations[46,47] of this general philosophy, it is usually assumed that the excited states decay isotropically in their c.m.s. into secondary particles, the number of which, $n_s(M)$, is proportional to the mass of this state, i.e., the decay is described by the statistical model. The kinematic characteristics of the final particles are completely fixed if one also specifies the relative motion of the excited systems or

[4)]Models of this type had also been proposed by previous authors,[43,49] who, however, generally considered only "isobar" excitation of the colliding particles and did not discuss the important consequence of scaling of the distributions in the fragmentation region ("limiting fragmentation").

(equivalently) the probability of exciting them up to a given value of the mass M. This probability $\rho(M)$ is usually taken[46,47] to be proportional to M^{-2}, so that the total average multiplicity $\langle n\rangle$ rises logarithmically with the energy:

$$\langle n\rangle \sim \int^{\sim\sqrt{s}} \rho(M)\, n_s(M)\, dM \sim \int^{\sim\sqrt{s}} M^{-2} M\, dM \sim \ln s. \qquad (4.1)$$

As a rule, no dynamical explanation of this behavior of the quantities ρ and n_s is given, so that this description is a purely phenomenological one.

We note that the dependence of the multiplicity on the missing mass in reactions involving the excitation of only one of the particles is given by the function $n_s(M)$ and is very different from the behavior of $\langle n\rangle$, whereas the dependences of these quantities are very similar experimentally.

These models are characterized by the presence of long-range correlations at asymptotic energies.

Another characteristic feature of fragmentation processes is clear from the qualitative picture in which two clusters are emitted: even if the average multiplicity has a weak growth with energy, there should be large fluctuations in the individual events.[45-47] In fact, the second correlation coefficient

$$f_2 = \langle n(n-1)\rangle - \langle n\rangle^2 \sim \int^{\sim\sqrt{s}} \rho(M)\, n_s^2(M)\, dM \sim \sqrt{s} \qquad (4.2)$$

rises rapidly with energy, i.e., the dispersion of the multiplicity distribution is large. Such a rapid growth of the dispersion with energy has not yet been observed experimentally.

These and several other characteristic results of the fragmentation model (for example, the probability of producing n particles has the form $\sigma_n \sim n^{-2}$) have led to the idea that concrete realizations of this model can be applied to the main types of inelastic interactions, if at all, only within a very limited range of energies[47] or, conversely, only asymptotically.[46] At the same time, fragmentation ideas are used in conjunction with reggeon exchange to describe diffraction dissociation reactions; we shall practically not consider such reactions at all in this review, since they belong to a special class of low-multiplicity processes which give a small contribution to the total cross section.

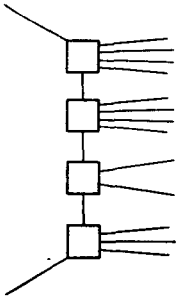

FIG. 13. Diagram for a multiperipheral process.

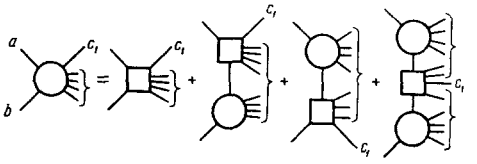

FIG. 14. Inclusive multiperipheral diagrams.

5. THE MULTIPERIPHERAL MODEL AND THE REGGEON SCHEME

The production of many centers of emission of particles is characteristic of the multiperipheral approach.[3,5,50,51] This is a consequence of the basic assumption that the momentum transfers are small. The process is represented diagrammatically in Fig. 13. In the case of an infinitely long multiperipheral chain at asymptotic energies, we can write an integral equation for the total cross sections σ:

$$\sigma = \bar{\sigma} + [\bar{\sigma}, \sigma], \qquad (5.1)$$

where

$$[\bar{\sigma}, \sigma] \approx \frac{1}{16\pi^3 s^2} \int \frac{dk^2 s_1\, ds_1\, s_2\, ds_2}{(k^2-\mu^2)^2} \bar{\sigma}(s_1, k^2)\, \sigma(s, k^2). \qquad (5.2)$$

The quantity $\bar{\sigma}$ is the cross section for non-peripheral reactions and can therefore include resonance production and elastic diffraction, as well as some of the inelastic processes. The integration goes over the squared masses s_1 and s_2 of the subsystems and the 4-momentum transfer k^2.

It is also easy to derive[52] equations for the inclusive spectra (for example, $F_1 = E\partial^3\sigma/\partial^3 p$):

$$F_1 = \bar{F}_1 + [\bar{F}_1, \sigma] + [\bar{\sigma}, F_1], \qquad (5.3)$$

where $\bar{F}_1$ is the inclusive spectrum of the vertex. The solution of this equation has the form

$$F_1 = \bar{F}_1 + [\bar{F}_1, \sigma] + [\sigma, \bar{F}_1] + [\sigma, [\bar{F}_1, \sigma]] \qquad (5.4)$$

and corresponds to a sum of contributions due to non-peripheral processes (the first term), fragmentation of the colliding particles (the second and third terms), and pionization (Fig. 14).

With this interpretation, Eqs. (5.1) and (5.3) correspond to a multi-component description of processes involving inelastic interactions. The advantage of the diagrammatic approach is that it not only provides a description of inelastic processes, but also relates their characteristics to the fundamental parameters of elastic scattering (and relates the inclusive spectra to the amplitude of the process $3 \leftrightarrow 3$). In particular, the logarithmic shrinkage of the diffraction peak of elastic scattering can be interpreted[53] in terms of an obvious picture of Brownian motion of the nodes in the diagram of Fig. 13 in the plane perpendicular to the collision axis, i.e., it is related to the logarithmic growth of the multiplicity with increasing impact parameter.

The principal results of the method are well known.

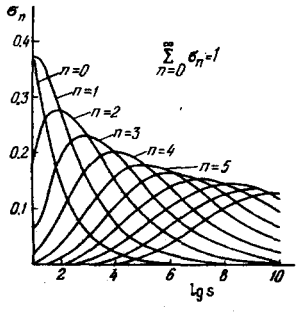

FIG. 15. Successive iterations in the ABFST model.

These results include a Regge behavior of the elastic scattering amplitude, a logarithmic growth of the multiplicity, scaling behavior and a plateau in the rapidity distribution, and short-range correlations. In general, all these predictions apply to the asymptotic energy region, where Eqs. (5.1) and (5.3) are valid and where it is easier for theorists to work.

At finite energies, only a finite number of iterations of Eq. (5.1) play a role, since all successive iterations vanish as a result of the conservation laws. The number of iterations and their energy dependence have a strong dependence on the form of the cross section $\bar{\sigma}$ for non-peripheral processes. This can be clearly seen by comparing Fig. 15, which shows the rapid change of successive iterations when $\bar{\sigma}$ is chosen in the form of a low-energy resonance (the ρ meson), with Fig. 16, where there is practically no change in the iterations (there are only threshold effects); this is so because non-peripheral processes, apart from resonances, include elastic scattering and the production of heavy clusters.

Thus the multiperipheral picture can include the production of an ever-increasing number of clusters, each of which decays into a fixed (energy-independent) number of particles,[50] as well as a practically constant relation between the channels with different numbers of clusters, whose masses rise with increasing energy,[54] a feature which is reminiscent of fragmentation ideas. Specific characteristics of inelastic processes at a given energy must be calculated by computer (see Ref. 5 for a review of models aimed at a quantitative description of the experimental data). The principal results and their comparison with the data are discussed in Sec. 7.

The foregoing scheme based on Eqs. (5.1) and (5.3) requires to some extent a phenomenological choice of the energy dependence of the cross section $\bar{\sigma}$ for non-peripheral processes (and the spectra $\bar{F}_1$). Moreover, the diagrammatic structure of $\bar{\sigma}$ is usually not specified.

We can provisionally distinguish two approaches

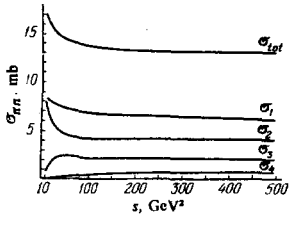

FIG. 16. The behavior of the iterations in the multiperipheral model when allowance is made for high-energy contributions in the blocks of the diagram.

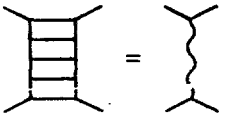

FIG. 17. The simplest diagrammatic interpretation of reggeon exchange.

among theoretical attempts to understand non-peripheral processes. In the first approach, the secondary interactions between the produced particles are regarded as being of paramount importance. Studies are made of "net" diagrams (see, e.g., Ref. 55) or of multiple scattering of the particles from the decays of clusters.[56] In particular, it has been pointed out[56] that the physical origin of the secondary interactions is the slow relative motion of the clusters and hence a strong overlap of the wave functions of the particles produced in different clusters. The interaction is so strong that the finite system can be thermalized, and the description of the process may go over from the multiperipheral picture to a thermodynamic picture. Thus the multiperiphery determines only the initial stage of the process in this case, and non-peripheral processes play a major role (corresponding to the non-homogeneous term in Eq. (5.1) and peripheral diagrams with heavy blocks). We can therefore classify the entire scheme of this type mainly according to the statistical-hydrodynamic picture, in which the initial conditions are determined by the multiperiphery (and not phenomenologically, as, for example, in the statistical bootstrap[24,33]). So far, however, this approach has not progressed far from the initial formulation of the problem.

At the same time, there has been an intensive development of another approach, in which the secondary interactions of the particles are relatively weak and multiperipheral in character. This is the so-called reggeon approach to the scattering problem. In the leading approximation, the conclusions of this approach follow from the multiperipheral character of inelastic processes, and multiple scattering (allowance for non-peripheral processes) leads only to correction terms.

Multiperipheral dynamics, which assumes that the principal mechanism of inelastic processes is the iteration of the low-energy interactions in the crossed (t) channel, is usually associated with the exchange of a Regge pole (in particular, the pomeron) in the elastic scattering amplitude. Therefore, if we replace the "ladder" by a reggeon (Fig. 17), we can make use of all the information about the properties of reggeons obtained from two-body and quasi-two-body reactions. It is well known[2,57] that the inclusive cross section for the reaction $AB \to C + X$ in the fragmentation region described by the diagram a in Fig. 18 has the form

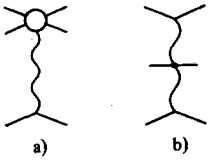

FIG. 18. Inclusive reggeon diagrams in the fragmentation region (a) and in the pionization region (b).

$$\frac{d\sigma_{AB}^{C}}{dy} \sim g_{AB}V_{A\bar{C}}(y)\exp[(\alpha(0)-1)Y] \qquad (5.5)$$

(where y is the rapidity, $Y \sim \ln s$, the factors g and V denote the vertices in Fig. 18, and $\alpha(t)$ is the exchanged Regge trajectory), which in the case $\alpha(0)=1$ leads to limiting fragmentation:

$$\frac{d\sigma_{AB}^{C}}{dy} \sim g_{AB}V_{A\bar{C}}(y)+O(s^{-1/2}) \qquad (5.6)$$

with an accuracy up to terms of order $s^{-1/2}$ (due to the Regge trajectories nearest to the vacuum trajectory).

In the pionization region (Fig. 18b), we have

$$\frac{d\sigma_{AB}^{C}}{dy} \sim g_{A}g_{B}V_{\bar{C}}\exp[(\alpha(0)-1)Y], \qquad (5.7)$$

which in the case $\alpha(0)=1$ gives a plateau in the rapidity distribution:

$$\frac{d\sigma_{AB}^{C}}{dy} \sim g_{A}g_{B}V_{\bar{C}}+O(s^{-1/4})+O(s^{-1/2}) \qquad (5.8)$$

with an accuracy up to the terms of order $s^{-1/4}$ (again due to the trajectories nearest to the vacuum trajectory). The kinematic corrections to Eqs. (5.6) and (5.8) are of order $O(s^{-1/2})$. The corrections due to the diagrams of Fig. 18b containing two non-vacuum reggeons with $\alpha_f(0)\approx 0.5$ or a pomeron and a trajectory with $\alpha(0)$ close to zero are of the same order.

The plateau in the rapidity distribution is also used in the parton picture, in which the transition of a particle into partons is given by the diagram of Fig. 19, where the energy of each successive parton is smaller than that of the preceeding one by a constant factor. Equation (5.8) leads to a logarithmic growth of the average multiplicity (for $\alpha(0)=1$):

$$\langle n\rangle = \frac{1}{\sigma}\int \frac{d\sigma}{dy}dy = aY+b. \qquad (5.9)$$

The equations for the two-particle correlations have the form

$$C_2(y_1, y_2) \sim \exp(-\beta\,|\,y_1-y_2\,|), \qquad (5.10)$$

where $\beta=1-\alpha_f(0)$, and $\alpha_f(0)$ is the Regge trajectory nearest to the pomeron ($\beta=0.5$ if $\alpha_f(0)=0.5$, and there are short-range correlations; β is small if cuts near the pomeron are important, and there are no short-range correlations).

Correction terms in the reggeon approach[58,59] arise when allowance is made for processes involving the exchange of two (Fig. 20a) or more reggeons or for the interaction of reggeons. Various types of inelastic processes which contribute to the two-reggeon diagram are represented by the diagrams b–d in Fig. 20. The diagram 20b gives the contribution of the (negative)

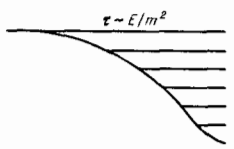

FIG. 19. A parton "ladder."

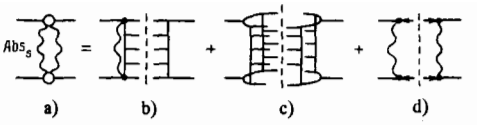

FIG. 20. The contributions of various inelastic processes to the two-reggeon diagram for the total cross section.

absorptive corrections to the basic processes of Fig. 17, the process 20c has twice the density in the rapidity of the secondary particles, and the diagram 20d describes processes with a gap in the rapidity distribution of the secondary particles.

The relative magnitudes of the contributions from the various inelastic processes to the total cross sections and the inclusive distributions are given by the AGK rules,[60] which were derived by considering the absorptive parts of the multi-reggeon diagrams. In particular, the contributions to the total cross section from the diagrams b, c, and d of Fig. 20 are in the ratio $-4, +2, +1$. According to the AGK rules, to calculate the single-particle inclusive distributions in the central region of the spectrum it is sufficient to take only the cut of the single-reggeon exchange, while the contributions from all higher-order exchanges cancel one another. Similarly, to calculate the two-particle correlations it is sufficient to take into account the contributions from the cuts of one and two reggeons (the situation is more complicated here in the presence of reggeon interactions; see Refs. 60 and 61). Explicit but simplified prescriptions for calculating all the characteristics of inelastic processes in the central region of the spectrum are given by the eikonal approach,[62] in which the distribution in the number of rescatterings is fixed by the phase of elastic scattering; the criterion for the applicability of this approach is the presence of well-distinguished "leading" particles.

Since the cross sections σ_{el} and σ_{dd} for elastic scattering and for diffusion dissociation are small ($\sigma_{el}/\sigma_{tot} \sim \sigma_{dd}/\sigma_{tot} \sim 1/5$), it is assumed that the cut contributions are relatively small and can be taken into account as a perturbation for hadronic interactions at currently accessible accelerator energies. The parameters which appear in the theory can be taken from experiment. The characteristics of the pomeron and its couplings with hadrons are extracted from the data on elastic scattering. The situation is more complicated as regards the parameters of the reggeon interactions. Allowance is usually made only for the triple-pomeron interactions. In this case, the (negative) corrections to the original triple-pomeron vertex r (due to absorption and to higher orders) are very large.[63,64] This requires that r takes a comparatively large (and poorly determined) value if use is made of the small effective value r_{eff} taken from the experimental data on inelastic diffraction production, and this in turn casts doubt on the quantitative estimates.

To give some idea of the role played by the various corrections to the single-pomeron exchange, we quote estimates[65] of the contributions from more complex diagrams to the pp interaction cross section at ISR

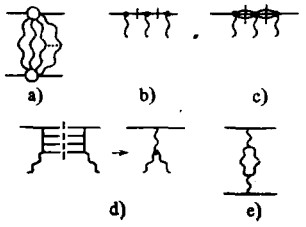

FIG. 21. Various types of corrections to single-pomeron exchange.

energies. The main (negative) correction (~30%) comes from multi-reggeon exchanges (Fig. 21a). These diagrams are dominated by the eikonal graphs, i.e., by elastic rescatterings (Fig. 21b). Diffractive excitation of small masses (Fig. 21c) modifies the eikonal contribution by about 30%. The excitation of large masses is described by the triple-pomeron graph (Fig. 21d), whose contribution to the cross section is close to 2 mb. Diagrams containing reggeon loops (Fig. 21e) give negligibly small contributions. It should be borne in mind that these estimates are at best semi-quantitative. They were quoted here in order to show what corrections might be expected in the multiperipheral scheme.

The observed growth of the cross sections at FNAL and ISR energies (see Fig. 1) has stimulated the development of models[65–69] in which the initial Pomeranchuk pole lies above unity: $\alpha(0)=1+\Delta_0>1$. The values of Δ_0 given by various estimates (whose uncertainties are due to the difficulty of correctly taking into account the triple-pomeron vertex, etc.) lie in the range between 0.06 and 0.15. The simplest dependence of the cross sections has the form[5)]

$$\sigma\sim s^{\lambda_0}, \quad \text{or} \quad \sigma\sim c(1+\Delta_0\ln s) \tag{5.11}$$

and

$$\frac{1}{\sigma}\frac{d\sigma}{dy}\Big|_{y=0}\approx\text{const}. \tag{5.12}$$

From the theoretical point of view, it is of interest to sum the reggeon diagrams in the asymptotic (or preasymptotic) energy region and to use the theory to extract information about the asymptotic behavior of the cross sections and the characteristics of multiparticle production. In this connection, there has been great interest in recent years in a field-theoretic formulation of reggeon theory (the RFT formulation; see Refs. 58 and 59 and the reviews[72]), which makes it possible to carry out calculations using contemporary methods of field theory (the renormalization group, continuation in the dimensionality of space, etc.[6)]). A "scaling" solution has been found,[74,75] corresponding to a position of the non-renormalized pomeron at the point $\alpha(0)=\alpha_c>1$[7)]. In this regime, the renormalized value of $\alpha_{out}=1$ and

$$\left.\begin{aligned}&\sigma_{tot}\sim(\ln s)^{\eta},\\ &\frac{d}{dt}\left(\ln\frac{d\sigma_{el}}{dt}\right)\sim(\ln s)^{\nu},\\ &\langle n^k\rangle\sim(\ln s)^{k(1+\eta)},\end{aligned}\right\} \tag{5.13}$$

where the values obtained[74–78] for the "critical indices" η and ν by different methods (the ε-expansion, an expansion in the number of loops, or the formulation of reggeon theory on a lattice) are similar ($\eta=1/6$ and $\nu=13/12$ to lowest order of the ε-expansion). Calculations were also made[79,80] of the form of the diffraction peak of elastic scattering (the relative value of the secondary maximum in this case was found to be 10^{-6}, which is surprisingly close to the result from the ISR data) and of the cross section $d^2\sigma/dtdM^2$ for inelastic diffraction. There is hope that this scaling solution can be "matched" to the result of perturbation theory in the number of pomeron interactions, and the region in which there is a change of regimes has been estimated as 10^{14}–10^{15} eV.[79–81]

It is not clear at the present time whether the ISR data correspond to the value α_c (see Refs. 64 and 70). If $\alpha<\alpha_c$, the renormalized value is $\alpha_{out}<1$; it has been argued[82,83] that the case $\alpha>\alpha_c$ also gives $\alpha_{out}<1$, i.e., that the cross sections must fall off at super-high energies of $\alpha\neq\alpha_c$.

For energies that are not super-high (but possibly far beyond present accelerator energies), it is possible to sum all the three reggeon diagrams (assuming that $\alpha(0)>1$).[84,85] The impact-parameter representation then leads to a picture of a gray disk with a logarithmically rising radius[86]:

$$\sigma_{tot}\sim\ln^2 s, \quad \langle n\rangle\sim\ln^2 s \tag{5.14}$$

and the moments of the multiplicity distribution satisfy the conditions of KNO scaling. There have also been arguments[69,87] that a further increase in the energy should lead to a Froissart regime with a power-law growth of the multiplicity and the inclusive cross section in the central region of the spectrum,

$$\langle n\rangle\sim\frac{s^{\lambda}}{\ln s}, \quad \frac{d\sigma}{dy}\Big|_{y=0}\sim s^{\lambda}, \tag{5.15}$$

and that KNO scaling should be violated.

It seems to us that reggeon field theory is mainly of theoretical interest at the present time. Its quantitative results can hardly be compared directly with the experimental data, in view of the major role played by the previously mentioned threshold effects, the phenomenological form factors, the uncertain effects due to the interactions and decays of secondary particles, etc. We therefore confine ourselves here to a qualitative description of the main observable effects which are obtained when allowance is made for multireggeon (or, in general, multiple) interactions.

When allowance is made for multiple interactions, the principal qualitative modifications of the multiperipheral model involve a suppression of the cross sections as a result of absorptive corrections, an increase in the

[5)] Equation (5.11) must be used with a value $\Delta_0\approx0.07$ in order to fit the growth of the total cross sections (by 7% in a unit interval of ln$s$; see Fig. 1). The correction diagrams containing the triple-pomeron interaction generally give a small growth of $(1/\sigma)d\sigma/dy$ at ISR energies.[68]

[6)] We mention another variant (the CRFT formulation; see Refs. 61 and 73) of reggeon field theory, which is based on a general topological classification of the diagrams and the utilization of the unitarity condition in the direct channel of the process.

[7)] It is estimated[65] that $\alpha_c-1\sim10^{-3}$, which gives a value much less than $\Delta_0\sim0.1$.

average multiplicity, a broadening of the original multiperipheral distributions in the multiplicity, and the appearance of long-range correlations between the momenta of the secondary particles. In particular, according to the eikonal model, the average number of particles $\langle n \rangle$ and the dispersion D of the distribution in the number of particles are changed from the original (multiperipheral) values $\langle n_1 \rangle$ and D_1 as follows (where no allowance is made for the conservation laws):

$$\begin{aligned} \langle n \rangle &= \langle n_1 \rangle \langle m \rangle, \\ D^2 &= \langle m \rangle D_1^2 + \langle n_1 \rangle^2 (\langle m^2 \rangle - \langle m \rangle^2), \end{aligned} \tag{5.16}$$

where m is the number of inelastic rescatterings. The multiplicity distributions obtained in this way can give a good fit to the experimental data in the case of an initial Poisson distribution[88] (see also Refs. 89 and 90).

Similarly, the correlation functions of the inclusive distributions are modified. The normalized correlation function R is given by

$$R(y_1, y_2) = \frac{1}{\langle m \rangle} R_1(y_1, y_2) + \frac{\langle m^2 \rangle - \langle m \rangle^2}{\langle m \rangle^2}, \tag{5.17}$$

where the second term, as in (5.16), is due to multiple scattering. Allowance for such terms improves the agreement with the experimental data.[91]

The change in the distributions in this case is a direct consequence of the possibility of processes involving interactions of different multiplicities. The resulting long-range correlations ($D^2 \gtrsim \ln^2 s$ and $f_2 \gtrsim \ln^2 s$) therefore have a "fictitious" statistical character, which is a result of taking an average over different possibilities. This feature is inherent in all multi-component models of multiple-particle production (in particular, models involving the production of clusters), in which an average is taken over different types of processes. This mechanism should be responsible for the observed decrease in the correlations in semi-inclusive processes,[92] where a selection is made, for example, of events with a fixed multiplicity, i.e., of processes which are predominantly of a single type.

Allowance for the law of energy-momentum conservation leads to a decrease in the number of particles at the edges of the spectrum and to additional obvious correlations[70] in the presence of multiple exchanges. The production of particles from several multiperipheral chains (see Fig. 20c) gives an increased multiplicity, while the leading particles (as well as each of the chains) have a reduced energy. Events with an enhanced density of secondary particles should therefore be characterized by a rapidity distribution with a reduced width and a smaller value of the variable x for the leading particles.

It should be noted that the effects described above follow from the existence of multiple interactions in the direct channel and are not directly associated with the reggeon concept. The reggeon calculus is merely the most popular and best developed general scheme for taking such effects into account.

As mentioned previously, the cut contributions to the total cross section are negative according to the reggeon rules, i.e., they are due to an interference between the multi-particle amplitudes; in particular, the multiple-scattering amplitude interferes with the ordinary multiperipheral amplitude (see Fig. 20b). One might attempt to take into account this interference directly in terms of the multiperipheral equation (5.1). The simplest model[93] leads to a decrease in the coefficient of the integral term (5.2) as a result of this interference by approximately a factor $\sigma_{tot}/\sigma_{inel}$. The multiple-scattering processes are then eliminated from the non-peripheral term $\bar{\sigma}$. If the coefficient in front of the integral term in (5.1) is regarded as a free parameter, the multiperipheral scheme is even more reminescent of multi-component models, in which the contributions of the various processes are determined from a comparison with experimental data.[94]

The problem of determining the contributions of the various processes is closely related to questions regarding the nature of the enchanged particles and the blocks at the nodes of the multiperipheral diagram. The nature of the t-channel exchange can be revealed, for example, in exclusive reactions[95] by separating the particles with definite quantum numbers ($\bar{p}$, Λ, etc.).

The character of particle emission at the nodes of the multiperipheral diagram is important for an understanding of the production mechanism and determines the correlation properties of the process. There exist schemes in which the entire set of resonances is exchanged and only resonances are produced,[96] as well as schemes which take into account pion exchange and resonance production[97-99] or, in addition, the production of fireballs.[5,100,101] These schemes lead to different correlations between the particles.

The simplest qualitative estimates of the correlations have been made in the model of independent cluster emission.[102-105] The rapidity distribution of the clusters is usually taken in the form of a "plateau," and their decay is either of the resonance type (when the distribution in the number of particles is given by a δ-symbol) or of the fireball type (a Poisson distribution). The conservation laws are taken into account only approximately.

The main conclusion is that this simplified model provides a qualitative description of most of the experimental data if it is assumed that the clusters decay on the average into at least 3 or 4 particles. We shall discuss this problem in greater detail in Sec. 7C.

6. QUARK MODELS

Models of multi-particle production based on information about the internal (quark) structure of the particles are of special interest. These models enable us to make use of information on deep inelastic lepton-proton interactions.[106] Quark models are not so well developed as the multiperipheral model or the statistical model, and they can give comparatively few quantitative results at the present time. They serve, however, to reveal the fundamental mechanisms of the processes.

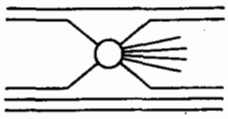

FIG. 22. Quark diagram for an inelastic πp interaction.

These models differ from one another mainly with regard to the role played by the gluons in production processes.

The simplest quark model is the additive quark model[107] applied to production processes[108] without explicit allowance for gluons. It is assumed here that the process takes place according to diagrams such as that of Fig. 22.

This model can account for a number of characteristic features of production processes[109] (such as KNO scaling[110]) and provides a number of specific predictions. The crucial predictions of this model are connected with the fact that the symmetric (forward-backward) system of the secondary particles produced in the central region of the spectrum is the c.m.s. of two interacting quarks, which for πp or Kp collisions is not the same, on the average, as the c.m.s. of the colliding hadrons. Experiments at energies of tens of GeV seem to confirm the existence of such a "quark–quark symmetric coordinate system."

An asymmetry of πN interactions in the c.m.s. has been observed in cosmic-ray data (see the discussion in Refs. 109 and 111) up to 600 GeV and is now confirmed by the FNAL data. If the symmetric system of the secondary particles were found to coincide with the overall c.m.s., this would be a strong argument against the additive quark model.

On the basis of these ideas, detailed calculations have been carried out of the relative multiplicities of secondary particles[112–118]; these calculations actually made use of only $SU(6)$ combinatorics and the assumption of statistically independent production and redistribution of the quarks. When allowance was made for a suppression in the production of strange quarks (by about a factor of two), it was possible to fit the observed relative multiplicities in the central region of the spectrum, their energy dependence, and the yields of various particles with large transverse momenta.

According to an alternative approach,[102,117,118] particle production in the central region of the spectrum is attributed to the gluon-gluon interaction, while all the valence quarks go through freely and are responsible for the flat energy spectrum of the leading particles in non-diffractive inelastic processes. This approach is based on the observation that the flat spectrum of these leading particles is in agreement with the rapidly falling quark spectrum found in deep inelastic lepton-proton processes. This model can also explain (although in a less natural way) the value of the cross section for diffraction dissociation, which is regarded as a shadow process due to the presence of "genuinely inelastic" gluon–gluon interactions.

A somewhat different role is ascribed to the gluons when it is assumed[119] that the gluons in the collisions are transformed into $q\bar{q}$ pairs, which enchance the quark sea. The quarks from the $q\bar{q}$ pairs are then redistributed, forming the final particles, as in Ref. 112. This is the first attempt to provide a global quantitative description of the multi-particle production process on the basis of the quark model (using Monte Carlo calculations).

The most remarkable feature of quark models[102,109,117–119] is that they demonstrate the possibility of a description of electromagnetic, weak, and strong interactions on the basis of a single set of distribution functions for the quarks in a proton. It has been argued[120] that the strong quark–quark interaction with small momentum transfer might explain the universal jet structure of production processes at high energies.

7. COMPARISON WITH THE EXPERIMENTAL DATA

Although each of the groups of models which we have considered is intended to describe the experimental data,[8)] the most complete quantitative comparisons have been made for the hydrodynamic model with the equation of state $p \approx \varepsilon/5$[25,26,31] and for the multi-fireball model.[5,101,121–123] We therefore chose to begin with these models, which differ markedly in their assumptions and methods, and attempted to compare them by showing which experimental characteristics they describe (see Table I). The main conclusion which this table suggests at first sight is that the inclusive distributions at energies up to hundreds of GeV are not very sensitive to the choice of the model (recent data on the growth of the inclusive cross sections at $x=0$ in the FNAL–ISR energy range may be more significant). Not all the characteristics listed in Table I are independent (for example, $\langle n\rangle\sigma = \int (d\sigma/dy)dy$, etc.). We shall consider only those characteristics which are most accurately known or which are most sensitive to the choice of the production mechanism.

A. The total cross sections

These simplest and most accurately measured quantities (see Figs. 1 and 2) are perhaps the ones which are mostly poorly described theoretically. Statistical-hydrodynamic models are not intended for calculations of the total cross sections at all. With a reggeon interpretation, the experimental data on the energy dependence of the cross sections determine our theoretical ideas about the leading and nearest Regge singularities and help to define the parameters of multiperipheral inelastic processes.

Thus the decrease of the cross sections in the region of tens of GeV required the introduction of the P' trajectory ($\alpha_{P'}(0) \approx 0.5$), and their slow growth over the interval 100–2000 GeV led to the scheme in which the initial leading pole lies above unity (in particular, fits to the experimental data on the total cross sections give a value for Δ_0 in Eq. (5.11) equal to ≈ 0.06–0.08).

[8)] We shall discuss here only hadron–hadron interactions. The specific properties of processes involving nuclei are considered in the next section.

The relationship between these results and the parameters of inelastic processes in the framework of the multiperipheral approach was discussed in Refs. 5 and 121, where it was shown how the parameters of the P and P' trajectories fix the inelastic characteristics of the process. The theoretical predictions about the dependence of the cross sections at higher energies differ appreciably from one another (see Sec. 4), so that they cannot be regarded as sufficiently reliable. The asymptotic behavior of the cross section in the eikonal approach can vary within wide limits, depending on the spin of the particles which mediate the interaction[124]—from a constant ($\sigma_{tot} \sim$ const) to the limiting Froissart behavior ($\sigma_{tot} \sim \ln^2 s$). Quark models can provide only relations between the cross sections for different processes. For example, according to the additive quark model, $\sigma_{pp}/\sigma_{\pi p} \approx 3/2$[107] (experimentally this ratio is $\approx 5/3$).

Thus experiment, and not theory, is in the lead in this field.

B. The inclusive distributions

The models are capable of giving a sufficiently good fit to the rapidity distributions at fixed energy (see Fig. 7).

An interesting problem here is raised by the experimental data[7] showing an appreciable growth with energy of the inclusive cross sections at $x=0$ in the FNAL–ISR energy region (see Sec. 2C) and Fig. 6).

For hydrodynamic models, in which there is no scaling ($\langle n\rangle \sim s^{1/4}$), this growth does not seem unnatural ($s^{1/4}$ varies by 60%). Statistical formulas of the type (3.3) successfully account for the composition of the secondary particles, i.e., the fractions of π, K, $\bar{p}$,[34,35,38] ρ,[38] $\bar{d}$, and He^3.[34,35] They also predict a growth of the fraction of heavier particles[34,35,38] (for example, $\langle n_{\bar{p}}\rangle/\langle n_\pi\rangle \approx c\langle n_\pi\rangle$ with $c=$ const), which is confirmed experimentally.[7]

An increase in the role of the pionization component at $x=0$ practically excludes further attempts to refine purely fragmentation models.

In the reggeon pole interpretation according to Eq. (5.8), we may attempt to eliminate a growth of the cross section by using expressions of the type

$$\frac{1}{\sigma}\frac{d\sigma}{dy}\Big|_{y=0} \sim \begin{cases} 1-\frac{d}{s^{1/4}}, & (7.1a) \\ 1-\frac{f}{s^{1/2}}. & (7.1b) \end{cases}$$

A fit to the ISR data requires $d \approx 2$ or $f \approx 9$, i.e., the correction terms at these energies are of the order of the main term and these formulas cannot be regarded as theoretically justified, although it is possible to obtain a fit to the data by formally combining terms of the type $s^{-1/2}$ and $s^{-1/4}$.

Primitive allowance for an increase in the number of ladders and for kinematic corrections (of the type $O(s^{-1/2})$ in the expressions (7.1)) has no noticeable effect. The situation might be improved by more accurate allowance for the conservation laws (as in Ref. 70), but this would imply that the simplest reggeon inclusive approach is unsuitable for making predictions at current accelerator energies. Moreover, an increase in the fraction of heavy particles is difficult to reconcile with a growth in the number of ladders, since the entire process would then tend to be more like processes at lower energies, where the fraction of kaons is reduced.

The situation is somewhat better in models involving the production of clusters having a sufficiently broad mass distribution (i.e., differing from resonances). If scaling is violated within a cluster, i.e., if there is a growth of $(K\sigma)_{cl}$, the product of the average multiplicity K in the cluster and its production cross section, then we can guarantee that there is a growth of the inclusive cross section.[52] The physical origin of the growth in the total and inclusive cross sections is then the process by which the clusters evolve (an increase in their mass and number as a function of energy). It is sometimes attempted to describe this process purely in terms of nucleon–antinucleon clusters.[125]

TABLE I.

Experimentally measurable characteristics	Statistics; hydrodynamics*)	Multiperipheral approach; Regge approach
Total cross sections	–	–
Multiplicity:		
1) $\langle n\rangle = f(s)$	+	+
2) Distribution and moments	+	+ (?)
3) KNO scaling	+ (?)	+ (?)
4) $n(\pi^0) = F(n^{ch})$	+ (?)	+
5) Composition	+	– (?)
Rapidity distribution:		
1) Pionization region	+	+ (?)
2) Fragmentation region	–	+
3) Energy dependence	+	+ (?)
4) Semi-inclusive	–	+
Distribution in p_T:		
1) Small p_T	+ (!)	+
2) Large p_T	+ (?)	+ (?)
3) Semi-inclusive	–	+
Distributions in pair masses and momentum transfers	–	+ (?)
Correlations:		
1) Dependence of p_T on p_L	+	–
2) Azimuthal	–	+
3) Two-particle, in rapidity	–	+
4) Multiparticle—rapidity intervals	–	+
5) Charge transfer	–	+ (?)
Inelastic diffraction	–	+

*)A plus sign indicates that good quantitative agreement with the data is obtained. A minus sign is used if: 1) the theory is not capable of giving the indicated characteristic, or 2) the results obtained seem unsatisfactory, or 3) calculations have not been performed. The symbols in parentheses indicate either additional arguments (or calculations) suggesting a good fit to the indicated characteristic (!) or doubts about the accuracy of the fit (?).

The idea of the approach to scaling from below as a result of an increasing density of the number of particles (in the rapidity variable) in the central clusters of the multiperipheral diagram has been discussed previously.[126]

Distributions in the transverse momentum of the type

$$\frac{dN}{dp_T^2} \sim \exp\left(-\frac{m_T}{T}\right), \tag{7.2}$$

where $m_T = \sqrt{p_T^2 + m^2}$, provide a good fit to the data for π, K, $\bar{p}$,[34,35,38] ρ, and ψ[37] for a single temperature T and are obtained in a natural way in the statistical approach (see Fig. 8). Experimentally, one can even observe a small deviation from the Boltzmann distribution (7.2) due to the Bose–Einstein statistics.[38] This deviation also shows up in theoretical calculations of the density of states of a relativistic ideal gas, applied to statistical models.[127] Thus the statistical formulas provide a good description of the limitation on the transverse momenta. This cannot be done by field theory and the diagrammatic (multiperipheral) method without introducing *ad hoc* form factors. However, numerical calculations with reasonable form factors lead to a fit to the experimental data.[5,121–123]

In the region of large transverse momenta, which we consider here only superficially, the most popular and varied models are the quark models (see Ref. 128 for further details). The emission of particles in the early stages of development of the system in the hydrodynamic approach explains the behavior of the spectra in p_T,[38,40,41] their energy dependence, and the growth in the fraction of heavy particles.[38] Further information about this stage can be obtained from the photon and lepton spectra.[129] A purely statistical description[130] can also succeed if the temperature of the system at the instant of decay depends on the total energy s and the critical volume V in the form $T \sim s^{1/2} V^{-1/4}$. In multiperipheral models, it is apparently necessary to resort to schemes[5,131] involving the production of more massive clusters, using the similarity of the properties of virtual pions and photons. The resulting simple picture, in which two mesonic clusters (jets) with large p_T and a system of mesons with small p_T (the "background") are produced, is in good agreement with the experimental results.[132] A simple "ladder" with resonance production is inconsistent with the experimental data, since it predicts that the multiplicity falls off with increasing p_T.[96]

To understand the production mechanisms, it is important to know the fractions of produced resonances. These are usually determined from the distributions in the pair masses. However, unlike quasi-two-body processes, multi-particle production involves a large number of false combinations, and the separation of the resonances is not very reliable. Therefore these data currently exclude only those schemes in which there are no resonances at all, leaving a rather large freedom in the magnitude of the resonance contribution (estimates of the fraction of ρ mesons vary from 20 to 70%).[133–137] Experiments in which leptons from the decays of resonances are detected may help to clarify the situation. The qualitative predictions of the models are that there are many resonances in quark models which take into account only the group-theoretic factors but not additional weight factors[112–115] and an appreciable number of resonances in the multiperipheral resonance ladder,[96] but fewer in the multi-cluster model[5,121–123] and in quark models with allowance for possible dynamical factors.[116,137]

C. Correlations and clusters

The separation of dynamical correlations from purely kinematic correlations connected with energy-momentum conservation is a difficult problem. The functions $C(y_1, y_2)$ and $R(y_1, y_2)$ which are usually employed (see Eqs. (2.12) and (2.13) and Fig. 9), with maxima at $y_1 = y_2$ indicating the production of particles by cluster groups, are not sufficiently simple. In the first place, the semi-inclusive correlations C_n and R_n (for a given multiplicity in the final state) have different reference levels (no correlations) for different n; secondly, the inclusive distributions contain strong interference terms from different values of n. Nevertheless, the conclusion that there are short-range correlations obtained from the relatively large value $R(0, 0) = 0.6$ (see Fig. 9)[97,102,103] remains valid when the semi-inclusive correlations are analyzed.[138–141] Estimates of the average number of particles in a cluster, based on calculations of the functions C and R in the model of independent cluster emission, lead to values of ~2–3 charged particles per cluster.[102–105,140–142]

The same values have been obtained by studying the rapidity gaps,[9,142] i.e., the distribution in the rapidity spacings between nearest-neighbor particles. It is easy to show that, for independent emission of clusters that decay into K particles and have a rapidity distribution with density ρ, the rapidity gaps Δy between nearest-neighbor particles obey the law[9,143]

$$\frac{dN}{dy} \sim \begin{cases} \exp(-\rho K \Delta y) & \text{for small } \Delta y, \quad (7.3) \\ \exp(-\rho \Delta y) & \text{for large } \Delta y. \quad (7.4) \end{cases}$$

The values of K quoted above were obtained by comparing these equations with the experimental data (Fig. 10). Although these estimates have been criticized and values twice as large for the number of particles in a cluster have been obtained from a fluctuation analysis,[144] it appears that the procedure used in the fluctuation analysis overestimates these values[145] as a result of long-range correlations.

Nevertheless, the inclusive distribution in the rapidity gaps is not very sensitive to the production mechanism,[10,101] since it is determined to a great extent by the multiplicity of the process. A distribution which is more sensitive to the mechanism is the semi-inclusive distribution in the rapidity intervals containing several particles,[10] i.e., the distribution in the quantities

$$\Delta y_{i,k} = y_{i+k+1} - y_i \tag{7.5}$$

(for $k = 0$ we have $\Delta y_{i,0} = \Delta y$), where i is the number of

a particle in an event according to its position in order of rapidity, and k is the number of particles inside the interval.[9)]

These distributions have a maximum (see Fig. 11) which moves towards smaller values of Δy as clusterization becomes more important,[143] and the most sensitive distributions are those with $k \sim n/2$ (where n is the number of particles in an event). Comparisons with experimental data[10,101] have made it possible to distinguish between different schemes that give practically the same results for the other characteristics, and it was observed that there may be an interesting structure in these distributions associated with the production of baryon clusters.

The study of quantities like $\Delta y_{i,k}$ with $k \neq 0$ implies a transition to multi-particle correlations. It is very difficult to do this by means of the usual generalization of the functions C and R, owing to the fact that it would then be necessary to consider a multi-dimensional rapidity space for a system of many particles.

A general conclusion which can be drawn from the correlation experiments is that we are certainly dealing with clusterization. It seems that clusterization does not lead simply to resonance production, but gives nontrivial multi-particle correlations; i.e., it involves the production of not only resonances, but also correlated groups of particles. Let us enumerate briefly the arguments in favor of this point of view:

1) The number of correlated charged particles is at least 2–3, whereas for resonances the value 2 is the absolute upper limit (the most probable value is $n^{ch} \sim 1.3$–1.5).[10)]

2) Various estimates give an effective cluster mass in the range 1.5 to 3 GeV, which is appreciably higher than the resonance masses of pionic systems (the probabilities of producing heavy resonances fall off sharply as a function of their mass).

3) The number of particles in a cluster rises as a function of the number n of particles in an event for $n > \langle n \rangle$; this indicates that the multiplicity distribution in a cluster is broader than the δ-function corresponding to resonance decay[138] (Fig. 23).

4) The coefficient in front of the logarithm of the energy in the behavior of the average multiplicity (see Eq. (2.2)) is small in schemes involving only resonance production).[11)]

5) The marked growth of the inclusive cross sections for producing K and $\bar{p}$ at ISR energies is inconsistent with a resonance "ladder" and requires the introduction of heavy clusters in the multiperipheral scheme.

Facts such as the violation of scaling at $x = 0$ after the onset of the growth in the cross sections and the behavior at large p_T can be explained qualitatively in the framework of the multiperipheral cluster model.

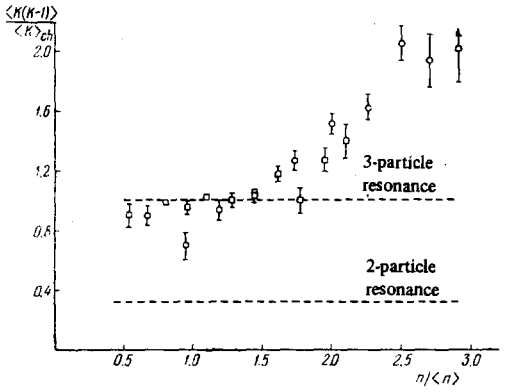

FIG. 23. The quantity $\langle K(K-1) \rangle / \langle K \rangle$ as a function of the number n of produced charged particles. The dashed lines show the dependence that would be obtained for production of only resonances decaying into two or three particles. The linear growth with n corresponds to a Gaussian distribution of particles in a cluster.

The experimentally observed suppression of charge exchange between groups of particles separated by large rapidity intervals[147] is also evidence in favor of the multiperipheral picture.[148]

Thus a reasonable combination of elements of the multiperipheral and statistical approaches, with a cluster mechanism for particle production, seems to be the best way of avoiding inconsistencies between the theoretical results and the experimental data.

8. INTERACTIONS WITH NUCLEI

The basic theoretical ideas about the mechanisms of multi-particle production processes in hadron–hadron collisions have also been widely used to describe hadron–nuclear interactions, with modifications to allow for the specific character of these interactions.

Practically all approaches now in use involve the assumption that there are two components in a hadron–nuclear interaction: a penetrating fast component, which takes approximately half of the energy and yields a small multiplicity, and a slower component, which interacts strongly with the nucleus and yields most of the produced particles. The existence of the penetrating component and the weakening of the interaction are usually explained by the fact that at high energies and small momentum transfers the longitudinal range of the interaction and the time of formation of the final state become large (see Refs. 149–151):

$$t_{eff} \sim l_{eff} \sim \frac{E}{m^2} \qquad (8.1)$$

and exceed the dimensions of the nucleus (see Chap. 9). However, the specific mechanisms and predictions of various models differ significantly from one another.

9) The distributions are obtained by summing over all possible values of the index i in each event.

10) The integrated contribution from resonances decaying into more than two particles is small.

11) Multiple interactions must be taken into account in such schemes (see Chap. 5).

A. The statistical-hydrodynamic approach

In the hydrodynamic approach, it is assumed that the interactions take place inside a tube of nuclear matter "cut out" by the incident hadron, which is considered as a whole.[152] The fast secondary particle is described by a hydrodynamic solution in the form of a plane wave, and most of the particles are produced by the passage of shock waves.[153] For an equation of state $p=\varepsilon/3$, calculations show that the average multiplicity on a nucleus A is given by[153]

$$\langle n\rangle_A \approx \langle n\rangle_p A^{0.19}. \tag{8.2}$$

The experimental data indicate a somewhat weaker dependence on A (see Eq. (2.15)). The spectrum of secondary particles in the hydrodynamic theory has an approximately Gaussian form in the variable y, which is consistent with the data, and the maximum of this distribution depends on the length of the tube (see Ref. 154). We note that the experimental data are consistent with a maximum of the inclusive distribution at the center of mass of the hadron-tube system (see Ref. 155).

Adopting a simplified thermodynamic treatment of the interaction between the hadron and the tube of nuclear matter, taking the equation of state $p=c_0^2\varepsilon$ (see Sec. III), we find that the average multiplicity has the dependence

$$\langle n\rangle_A \sim E_{\text{lab}}^{(1-c_0^2)/2(1-c_0^2)}\, A^{(1+3c_0^2)/6(1+c_0^2)}, \tag{8.3}$$

which differs somewhat from the result of a detailed calculation (Eq. (8.2)).

B. The multiperipheral parton approach

This approach to nuclear interactions is particularly simple if the process is considered in the antilaboratory system of coordinates.[156] The slow partons of the various nucleons of the rapidly moving and Lorentz-contracted nucleus must overlap spatially and, by virtue of of the basic assumption of local equilibrium of the parton distribution (see Ref. 151), should form a single "chain" of slow partons which interacts with the hadron (Fig. 24a).

From the point of view of the reggeon approach, this mechanism is equivalent to the dominance of the "fan" diagrams (Fig. 24b). A summation of these diagrams,[157,158] interpreted literally, gives a negligibly small correction to the total and inclusive cross sections at any reasonable energies if use is made of the standard parameters for the reggeons and their interactions (in particular, the triple-reggeon vertex r). Actually, the energies of those secondary particles (in the laboratory system) which are rescattered and reproduced (y_0 in Fig. 24b) are relatively low, and these energies are not high enough to speak of diagrams with

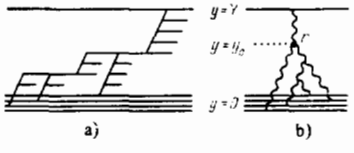

FIG. 24.

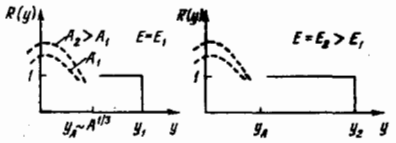

FIG. 25. The qualitative form of the ratio of the inclusive distributions for nuclei and nucleons in the multiperipheral parton scheme, as a function of the rapidity and the atomic number.

branching of the pomerons. It is more realistic to make a semi-phenomenological calculation of the processes of parton reproduction[159] with allowance for the conservation of energy.

In this picture, the single-particle distributions obey the obvious relations

$$R_A(y) \approx 1, \qquad Y > y > y_0, \tag{8.4a}$$

$$R_A(y) \approx \bar{\nu} \approx \frac{A\sigma_{hN}}{\sigma_{hA}}, \quad y < y_0, \tag{8.4b}$$

where $\bar{\nu}$ is the average number of chains. Thus the inclusive distribution in the multiperipheral parton scheme at sufficiently high energies must have the form shown schematically in Fig. 25. Accordingly, the quantity $R_A=\langle n_s\rangle_A/\langle n_s\rangle_p$ should tend to unity with increasing energy. Detailed calculations can be found in Ref. 159.

C. Multiple-interaction models

As we have already pointed out in Sec. 5, the main correction to the multiperipheral model for the hadron–hadron interaction comes from multiple scattering. Multiple-scattering effects play a much larger role in hadron–nuclear interactions.

Successful calculations of the integrated cross sections for interactions of relativistic particles ($E \gg m^2R$) with hadrons have been made using the Glauber approximation,[160] according to which the hadron–nucleon scattering phases are additive (corrections are usually added for inelastic rescattering).[161] This approximation can be derived in the framework of a general multiple-scattering formalism and the reggeon approach.[161–163]

We would like to point out that (contrary to the claims frequently encountered in the literature) the Glauber approximation, as formulated in the language of Feynman diagrams, does not imply successive interactions with the nucleons of the nucleus. This approximation can be derived in field-theoretic models[164] from the eikonal approximation (and is in fact equivalent to the latter), and it takes into account, for example, the set of Feynman diagrams of the type shown in Fig. 26, where P is an arbitrary initial block of the hadron–nucleon interaction (such as a Regge pole) containing multi-particle intermediate states. This approximation satisfies the

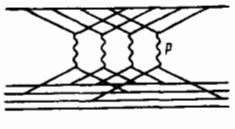

FIG. 26.

AGK rules for the contribution of the various inelastic intermediate states (see Ref. 165). Since the various contributions to the scattering phase in the eikonal approximation are additive, the total phase of the hadron–nuclear interaction can be written as a sum of the phases of the hadron–nucleon amplitudes, which is equivalent to the Glauber approximation. The AGK rules for partitioning the total hadron–nucleon amplitudes then apply (see Ref. 166).

The characteristics of interactions with nuclei are determined by the average number of interactions,

$$\bar{\nu} = \frac{A\sigma_{hN}}{\sigma_{hA}}. \quad (8.5)$$

The average multiplicity in the Glauber scheme should be proportional to $\bar{\nu}$ at super-high energies, $R_A \sim \bar{\nu}$, i.e., it approaches a dependence close to $A^{1/3}$, which is very different from the prediction of the multiperipheral scheme, in which $R_A \to 1$ as $E \to \infty$. The multiplicity is much smaller at existing energies, since the simultaneous production of particles from several blocks ("ladders") means that each of them has a small energy. The available experimental data for R can be fitted by a dependence of the form

$$R = \alpha + \beta\bar{\nu}, \quad (8.6)$$

where $\alpha \sim \beta \sim 0.5$. The distribution in the number of particles for interactions with nuclei is broader than in hadron–nucleon interactions. Calculations[167] carried out in the framework of the Glauber approximation can provide a fit to the available experimental data.

If no allowance is made for the law of energy conservation, the inclusive distribution in the central region of the spectrum is given by the expression

$$R_A(y) \approx \frac{1}{\sigma_{hA}} \sum_\nu n_\nu \sigma_\nu \frac{1}{n_1} \approx \frac{1}{\sigma_{hA}} \sum_\nu \nu\sigma_\nu = \bar{\nu}, \quad 0 \ll y \ll Y, \quad (8.7)$$

where σ_ν is the cross section for processes in which particles are produced in the ν blocks. Allowance for the conservation of energy should decrease this value somewhat. The conservation of energy acquires a very important role for rapidity values near the fragmentation region of the incident particle, where particles can be produced from only a single block:

$$R_A(y) \sim \frac{1}{\sigma_{hA}} n_1\sigma_1 \frac{1}{n_1} = \frac{\sigma_1}{\sigma_{hA}} < 1, \quad y \approx Y - \Delta. \quad (8.8)$$

As a result, the rapidity distribution of the secondary particles should have the form shown schematically in Fig. 27 (cf. Fig. 25). The available experimental data do not enable us to discriminate between the qualitative predictions of Figs. 25 and 27 with confidence. Little can be said about the fragmentation region of the nucleus (small y_{lab}). The slow particles produced in the tube, the number of which is expected to be proportional to $\bar{\nu}$, should be increased in number by the interactions with the nucleons of the nucleus, leading to an increase in the total number of secondary particles. A separate analysis is necessary for the fragmentation region of the incident hadron ($y \approx Y$), which receives contributions

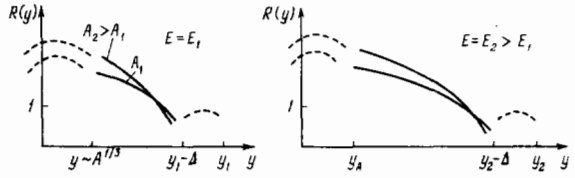

FIG. 27. The effect of multiple interactions on the behavior of the inclusive distributions (cf. Fig. 25).

from the particles due to diffraction dissociation of the hadron. We can expect that $R_A(y) \sim 1$ in this region.

We have not considered correlations of the secondary particles here, since the theoretical analysis of correlations in hadron-nuclear interactions is in its infancy.

In addition to the approaches considered above, we mention also models which consider the production of clusters in nuclear matter,[168] the evolution of the energy flux in the nucleus,[169] collisions with the nucleon tube,[170–172] the existence of two phases of hadronic matter,[173] etc. Unfortunately, the existing experimental data do not enable us to make an unambiguous choice in favor of any of these models.

9. THE SPACE-TIME PICTURE

To understand the mechanisms of multi-particle production, it can be useful to study the space-time picture of the interactions. Models which give similar momentum distributions may be very different from one another in their space-time characteristics. In the simplest geometrical picture, for example, we should expect a decrease in the impact parameter b to lead to an increase in the multiplicity. At the same time, the multiplicity given by a naive multiperipheral picture is increased by an increase in the length of the multiperipheral chain, corresponding to larger impact distances. These pictures can in principle be distinguished experimentally (the first proposal of this type was made in Ref. 174), thus making it possible to decide which models are applicable.

Space-time concepts are particularly important for an understanding of interaction processes in extended systems such as atomic nuclei. Different assumptions about the way in which the processes evolve in space and time lead here to very different predictions for the characteristics of multiparticle production. Conversely, a study of the characteristics of interactions with nuclei provides a unique opportunity of testing our ideas about the nature of the elementary interactions. For these reasons, the space-time description has received very great attention in recent years.

A number of models make explicit use of some particular space-time picture of the interaction. The standard hydrodynamic model is based on the concept of a Lorentz-contracted and expanding disk of hadronic matter; spherical symmetry is assumed in the statistical model (in the appropriate coordinate system). Such a picture can be obtained in field-theoretic models as follows.[175] The probability of any process can be written as

$$dW = \left| M(P, p_1, p_2, \ldots)\,\delta^{(4)}\left(P - \sum p_i\right)\right|^2 \prod_i \frac{d^3p_i}{2E_i}, \qquad (9.1)$$

where one of the δ-functions is interpreted as a product of the spatial volume and the total time of observation. Replacing the remaining δ-function by the integral $\int d^4x \exp[i(P - \sum p_i)x]$ and performing the integration over the final momenta of the particles, we can then extract the effective values x_{eff} for a given form of the matrix element M. This procedure gives correct results in the non-relativistic case and for the simplest field-theoretic models. When applied to the model of uncorrelated jets with a cutoff in the transverse momentum, it leads to a Lorentz-contracted volume, while in the case of the Fermi model it leads to a spherically symmetric volume.

At the same time, if we make use of the integral representation for the imaginary part of the elastic amplitude,

$$\operatorname{Im} M(p, p'; q, q') \sim \int d^4x e^{i(q+q')x/2} \langle p' | [j(x) j(0)] | p \rangle, \qquad (9.2)$$

and, for forward scattering, represent the exponent in (9.2) in the form $q_0(t-z) - q^2 z/2q_0$, we can determine the effective values of the longitudinal coordinate z by studying the cross section as a function of the virtuality of q^2.[178] The data on deep inelastic electroproduction indicate[177] that the main contribution to the elastic amplitude (9.2) comes from large longitudinal distances, $z_{eff} \sim q_0/m^2$.

The effective region of space-time in these examples was interpreted to mean the characteristic values of the coordinates contained in some particular integral representation for the probability of the process. This interpretation is in general ambiguous. The values of x_{eff} can be changed by identity transformations of the integrals or by choosing different expansion bases for the amplitude (expansions in the "bare" or real fields).[178] Moreover, we can distinguish different meanings of the spatial region, such as the region of interaction with the target or the region in which the secondary particles are formed. In the multiperipheral parton model, for example, the hadron at each instant of time is a "sphere"[153] (Fig. 28) of radius $\sim 1/m$ (and transverse dimensions $\sim \sqrt{R^2 + \alpha' \ln E}$) determined by the slowest parton (the interaction region), with internal contracted shells of faster partons (the region of highest energy density); the time of evolution of the parton ladder and the corresponding longitudinal distance are large, $z_{eff} \sim E/m^2$ (the formation region; see Fig. 19). It has also been proposed[179] to regard the hadron as a parton state of length $\sim E/m^2$. On the whole, it is necessary to rely mainly upon intuition in the space-time description of these processes. A major role is played here by large times and longitudinal distances $\sim E/m^2$.

Large longitudinal distances l_{eff} which grow with energy are important in a number of well-studied effects in electrodynamics.[180,181] The idea of a decisive role for large l_{eff} was also used successfully many years ago in the analysis of the strong interactions.[149,182] What seems to be of the greatest practical importance is the

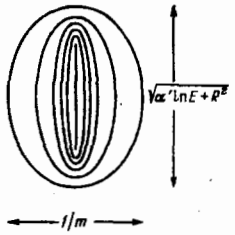

FIG. 28.

idea that the fast produced particles with momenta $\mathbf{p}_i$ approximately parallel to the initial momentum are formed as individual (spatially separated) real particles at large longitudinal distances of order p_i/m^2. Also of great interest is the description of a fast particle which undergoes an interaction as a "truncated" formation, whose interaction can become weaker at distances of order E/m^2 (see Refs. 150 and 183).

When applied to production processes in nuclei, the idea of a large formation time for the particles means in essence that the fast secondary particles are formed outside the nucleus (with $E_i/m^2 \gg R$), so that they do not lead to the effect of cascade multiplication. In the language of the parton model, this corresponds to the passage of the fast partons through the nucleus without interacting.[156,159] The existing experimental data on multiparticle production on nuclei, and in particular the small number of secondary particles emitted in the forward direction (see Sec. IIF), favor this interpretation; at any rate, these data exclude the simple cascade model. This point of view is also confirmed by the data on the effective interaction cross sections of the 3π and 5π systems produced diffractively in pion–nuclear collisions: these sections are anomalously small, $\sigma_{5\pi} \lesssim \sigma_{3\pi} \sim \sigma_\pi$.[184] We note also that the available data on the yield of fast protons in proton–nuclear interactions can be interpreted[185] on the basis of the assumption that the proton cross section is reduced after the first interaction in the nucleus; this supports the idea of a "truncated nucleon" whose character is restored after a time of order E/m^2. A direct experimental confirmation of the foregoing ideas would be of immense value for the theory of multiple-particle production at high energies and for strong-interaction physics as a whole.

Let us now consider the currently available results on the direct experimental determination of the dimensions of the interaction region. The effective transverse dimensions which characterize inelastic processes as a whole ($b_{eff} \sim 1$ F) are determined by means of the unitarity condition from the data on the elastic differential cross sections. The probabilities of inelastic interactions for various values of the impact parameter are shown in Fig. 29. The most peripheral processes are those of diffraction dissociation.[187–189]

The results referring to the individual exclusive processes are of greater interest. One of the methods of determining the interaction region is based on measurements of the momenta of the secondary particles. The lower limit of the values b_{eff} has been estimated[190–192] by means of the equation

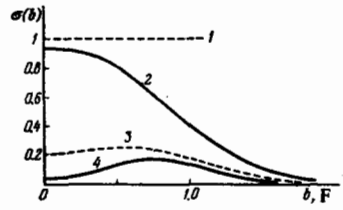

FIG. 29. The probabilities of inealstic processes for various values of the impact parameter. 1—the limit of total absorption ("black disk"); 2—total contribution of inelastic processes in pp interactions; 3—limiting value of the contribution of inelastic diffraction[186]; 4—the contribution of inelastic diffraction in pp interactions (according to Ref. 187).

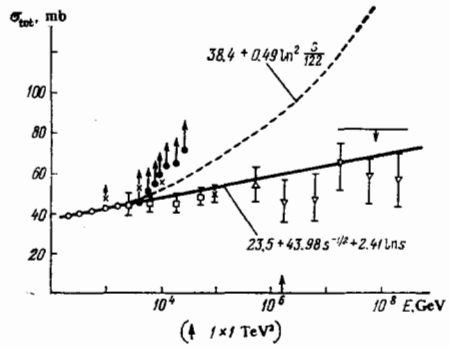

FIG. 30. Cosmic-ray data on the total cross sections.

$$\langle b^2\rangle \geqslant \frac{\langle\sum_i [x_i^2 - (k_{i\perp}^2/2p^2)]\rangle^2}{\langle\sum_{i,j} x_i x_j \mathbf{k}_i \mathbf{k}_j\rangle} \equiv b_L^2, \tag{9.3}$$

where p is the initial momentum, and x_i and $\mathbf{k}_i$ are the Feynman variables and the transverse momenta of the secondary particles (more precise estimates for $\langle b^2\rangle$ have recently been proposed).[193]

The principal results are as follows:

1) The value of b_L falls off by a factor 3–4 as the number of particles increases from 4 to 9, i.e., the multiplicity is greater for central interactions.

2) For a given multiplicity, b_L has a weak growth with energy.

3) Inelastic diffraction is characterized by increased values of b_L.

4) Processes involving the exchange of strangeness or baryon number occur with smaller values of b_L.

These results tend to support the naive geometrical picture of the interaction more than the multiperipheral picture of Brownian motion in the transverse plane. They can also be compared with the fact that the multiperipheral logarithms are in general much smaller than the contributions of the residues.

Another method of determining the region in which particle production takes place is to study the correlations of identical particles.[194–198] This method, taken from astronomy[199] (see also the earlier works),[200] is based on the existence of second-order interference effects for identical particles emitted at different instants of time and from different points of space. The width of the interference maximum is inversely proportional to the dimensions of the region in which the particles are emitted. If w/w_0 is the distribution of the number of observed pairs of identical particles in relation to the background (i.e., in relation to the number of pairs for which there is no interference effect), then in the region of the maximum we have

$$\frac{w(q)}{w_0(q)} \approx 1 + \exp\left(-\frac{1}{4} q_\perp^2 R^2 - q_0^2 \tau^2\right); \tag{9.4}$$

here q_0 and q_T are the differences in energy and transverse momentum of the two detected particles, R gives the transverse dimensions of their emission region with respect to the direction of observation, and τ is the characteristic scatter in the time, consisting of the average lifetime of the particle sources, the scatter in the instants of emission, and the delay time of the particles in traversing the various longitudinal distances.

Experiments[201–204] give a value $R \sim 1$ F and a relatively small value of τ ($c\tau < R$), in conflict with the concepts of large times and longitudinal distances. However, it must be borne in mind that correlation measurements provide information about intervals that are characteristic of the production of particles with neighboring momenta and that these intervals may be smaller than the total interaction range. A definitive interpretation of the results is therefore possible only in the framework of some particular model of the interaction.

On the whole, attempts to construct a space-time description of processes at high energy, and in particular ideas about the role of large effective distances, have raised a number of very interesting problems, which must be regarded as still open. The main hopes here rest on the study of interactions with nuclei and on the further development of experimental methods of directly measuring the interaction range.

10. VERY HIGH ENERGIES

What can we say about the applicability of our ideas about the mechanisms of multi-particle production in the region of very high energies?

Let us consider what the cosmic-ray data tell us:

1) The total cross sections rise relatively slowly with energy, if at all (Fig. 30).

2) The average multiplicity probably rises faster than logarithmically (Fig. 31).

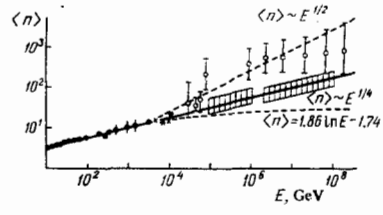

FIG. 31. Cosmic-ray data on the average multiplicity.

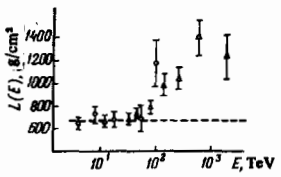

FIG. 32. The penetration depth of hadrons in lead as a function of energy.

We mention that there is as yet no consistent theoretical scheme in which, for example, the cross section rises logarithmically (but not like $\sim \ln^2 s$), while the multiplicity rises according to a power law (with a sufficiently large exponent).

3) Scaling in the quantity $(E/\sigma)d^3\sigma/d^3p|_{x=0}$ is evidently not observed. Calculations show[205] that the data of the Pamir experiment in the range of energies $10-10^3$ TeV favor a growth of the inclusive distributions Ed^3N/d^3p in the pionization region of small $|x|$, with a possible weak fall-off in the fragmentation region (i.e., the growth observed at the ISR up to 2 TeV persists at higher energies).

4) The absorption of the hadronic shower component falls off sharply at energies of about 10^{14} eV[206-209] (Fig. 32). If this is interpreted as a manifestation of a new penetrating component, its contribution in relation to that of the ordinary hadrons should be at least 25% at energies above 100 TeV.

5) The ratio of the energy of the electron-photon component to that of the hadronic component at the center of the shower rises from 0.8 to ~1.5 over the range of energies from 40 to 300 TeV.

The authors of Refs. 206-209 point out that these results can be interpreted in terms of the production and decay of some new particles into channels involving the production of electrons and photons, or possibly the associated production of new particles together with leptons and photons.

6) There exist individual exotic events. The most interesting events here are those involving the production of a large number of particles in a small rapidity interval, which can be interpreted as a manifestation of heavy clusters[210] of mass 25 GeV/c^2. We note that the possibility of clusters of smaller mass 3–4 GeV/c^2 has also been discussed long ago in cosmic-ray physics[211] (see also the review[11]).

Thus we can expect that the study of the energy region beyond 10^{14} eV will necessitate a re-examination of our ideas about the mechanisms of multi-particle production. Colliding beams of energy 1×1 TeV^2 would permit an intensive investigation of the beginning of this region.

11. CONCLUSIONS

In the past few years, since the introduction of the new generation of accelerators, multiparticle production processes have taken on a much greater role in particle physics. In this review we have attempted to outline the general situation regarding our current theoretical understanding of multiparticle processes, without touching upon a number of specific interesting processes such as the production of particles with large transverse momenta, deep inelastic scattering, and e^+e^- annihilation.

There is now a vast amount of experimental data on multiparticle production, and there have been many proposals of theoretical schemes, often only tenuously related to one another, which can account for the results of various groups of experiments. We have therefore strived to emphasize the qualitative predictions and those experimental characteristics which are most sensitive to the specific assumptions of the various models and which might help to select the most satisfactory theoretical schemes. We would also like to stress that each of the proposed models should be compared with the totality of available experimental data. Of course, this calls for extensive numerical work, generally requiring the use of a Monte Carlo method. However, in a number of cases such a test is decisive for the further assessment of a model.

In addition to the traditional models, a number of new approaches to multiparticle production processes have been developed in recent years, which may elucidate the general character of interactions at high energies. Here we would like to mention the application of the space-time picture of the evolution of the processes (Sec. 9) and the first attempts to make use of information about the internal structure of the hadrons (Sec. 6). There are new exciting possibilities connected with the region of super-high energies (Sec. 10). Cosmic-ray data provide evidence of a change in the character of particle interactions at energies of order 10^{14} eV. The authors are grateful to E. L. Feĭnberg for numerous discussions about the problems treated in this review.

[1]E. L. Feinberg, Phys. Rep. **5C**, 237 (1972).
[2]A. H. Mueller, in: Proc. of the 16th Intern. Conf. on High Energy Physics, Vol. 1, NAL, Batavia, 1972, p. 347.
[3]A. Bassetto, Fortschr. Phys. **22**, 225 (1974).
[4]I. L. Rozental', Usp. Fiz. Nauk **116**, 271 (1975) [Sov. Phys. Usp. **18**, 430 (1975)].
[5]I. M. Dremin and A. M. Dunaevskii, Phys. Rep. **18C**, 159 (1975).
[6]E. Albini, P. Capiluppi, G. Giacomelli, and A. M. Rossi, Nuovo Cimento **A32**, 101 (1976).
[7]K. Guettler, B. G. Duff, M. N. Prentice, *et al.*, Phys. Lett. **B64**, 111 (1976). C. Bromberg, T. Ferbel, P. Slattery, *et al.*, Nucl. Phys. **B107**, 82 (1976).
[8]L. Foa, Phys. Rep. **22C**, 1 (1975).
[9]C. Quigg, P. Pirila, and G. H. Thomas, Phys. Rev. Lett. **34**, 290 (1975). A. Krzywicki, C. Quigg, and G. H. Thomas, Fermi Lab-Pub.-75/40-THY, 1975.
[10]M. I. Adamovich, M. M. Chernjavskii, I. M. Dremin, *et al.*, Nuovo Cimento **A33**, 183 (1976).
[11]S. P. Denisov *et al.*, Nucl. Phys. **B61**, 62 (1973).
[12]D. I. Blokhintsev, Zh. Eksp. Teor. Fiz. **32**, 350 (1957) [Sov. Phys. JETP **5**, 286 (1957)].
[13]E. Fermi, Prog. Theor. Phys. **5**, 570 (1950); Phys. Rev. **81**, 683 (1951).
[14]I. Ya. Pomeranchuk, Dokl. Akad. Nauk SSSR **78**, 889 (1951).
[15]L. D. Landau, Izv. Akad. Nauk SSSR Ser. Fiz. **17**, 51 (1953).
[16]P. Carruthers and F. Zachariasen, Preprint LA-UR-75-375, 1975; Phys. Rev. **D13**, 950 (1976).
[17]F. Cooper and D. H. Sharp, *ibid.* **D12**, 1123 (1975).

[18]R. A. Milekhin, in: Trudy Mezhdunarodnoĭ konferentsii po kosmicheskim lucham (Proc. of the Intern. Conf. on Cosmic Rays), Vol. 1, Izd. Akad. Nauk SSSR, Moscow, 1960, p. 223.
[19]R. C. Hwa, Phys. Rev. **D10**, 2260 (1974).
[20]C. B. Chiu and K.-H. Wang, *ibid.* **D12**, 272 (1975). C. B. Chiu, E. C. G. Sudarshan, and K.-H. Wang, *ibid.*, p. 902.
[21]S. Eliezer and R. M. Weiner, *ibid.* **D13**, 87 (1976).
[22]R. Dashen, S. Ma, and H. J. Bernstein, *ibid.* 187, 345 (1969).
[23](a) A. I. Bugriĭ and A. A. Trushevskiĭ, in: Trudy XVIII Mezhdunarodnoĭ konferentsii po fizike vysokikh énergiĭ, Tbilisi, 1976 (Proc. of the Intern. Conf. on High Energy Physics, Tbilisi, 1976), JINR, Dubna, 1977, p. 23. (b) L. L. Jenkovszky and A. A. Trushevskiĭ, Preprint ITF-74-51E, Kiev, 1974.
[24]R. Hagedorn, Nuovo Cimento **35**, 216 (1965).
[25]É. V. Shuryak, Yad. Fiz. **16**, 395 (1972); Preprint 75-4, Inst. of Nuclear Physics, Siberian Division, USSR Academy of Sciences, Novosibirsk, 1975.
[26]O. V. Zhirov and É. V. Shuryak, Yad. Fiz. **21**, 861 (1975) [Sov. J. Nucl. Phys. **21**, 443 (1975)].
[27]M. I. Gorenshteĭn and G. M. Zinov'ev, cited in Ref. 23a, p. 23.
[28]P. Carruthers and M. Duong-van, Phys. Lett. **B41**, 593 (1972); Phys. Rev. **D8**, 859 (1973).
[29]F. Cooper and E. Schonberg, Phys. Rev. Lett. **30**, 880 (1973).
[30]F. Cooper and G. Frye, Phys. Rev. **D10**, 186 (1974).
[31]B. Andersson, G. Jarlskog, and G. Damgaard, Preprint TH2133-CERN, 1976.
[32]C. B. Chiu and K.-H. Wang, Phys. Rev. **D12**, 2715 (1975).
[33]J. Ranft, Nucl. Phys. **B105**, 139 (1976).
[34]I. N. Sisakyan, E. L. Feĭnberg, and D. S. Chernavskiĭ, Zh. Eksp. Teor. Fiz. **52**, 545 (1967) [Sov. Phys. JETP **25**, 356 (1967)].
[35]E. L. Feĭnberg, Usp. Fiz. Nauk **104**, 539 (1971) [Sov. Phys. Usp. **14**, 455 (1972)].
[36]E. I. Daĭbog, Yu. P. Nikitin, and I. L. Rozental', Yad. Fiz. **16**, 1314 (1972) [Sov. J. Nucl. Phys. **16**, 724 (1973)]; Izv. Akad. Nauk SSSR Ser. Fiz. **37**, 1396 (1973).
[37]T. F. Hoang, Phys. Rev. **13D**, 1881 (1976).
[38]É. V. Shuryak, Yad. Fiz. **20**, 549 (1974) [Sov. J. Nucl. Phys. **20**, 295 (1975)]; Phys. Lett. **B42**, 357 (1972).
[39]M. Chaichian, H. Satz, and E. Suhonen, *ibid.* **B50**, 362 (1974).
[40]J. J. Dumont and L. Heiko, Preprint IIME-74-1, Univ. of Brussels, 1974.
[41]M. I. Gorenstein, V. P. Shelest, and G. M. Zinoviev, Phys. Lett. **B60**, 283 (1976).
[42]T. T. Chou and C. N. Yang, Phys. Rev. **170**, 1591 (1968).
[43]E. L. Feĭnberg and D. S. Chernavskiĭ, Dokl. Akad. Nauk SSSR Ser. Fiz. **81**, 795 (1951); **91**, 511 (1953).
[44]R. K. Adair, Phys. Rev. **172**, 1370 (1968).
[45]J. Benecke, T. T. Chou, C. N. Yang, and E. Yen, *ibid.* **188**, 2159 (1969).
[46]R. Hwa, *ibid.* **D1**, 1790 (1970); Phys. Rev. Lett. **26**, 1143 (1971).
[47]M. Jacob and R. Slansky, Phys. Rev. **D5**, 1847 (1972).
[48]H. Cheng and T. T. Wu, Phys. Rev. Lett. **23**, 670 (1969).
[49]S. Takagi, Prog. Theor. Phys. **7**, 123 (1952).
[50]D. Amati, A. Stanghellini, and S. Fubini, Nuovo Cimento **26**, 896 (1962).
[51]F. Zachariasen, Phys. Rep. **2C**, 1 (1971).
[52]I. M. Dremin and A. M. Dunaevskiĭ, Yad. Fiz. **22**, 568 (1975) [Sov. J. Nucl. Phys. **22**, 294 (1975)].
[53]E. L. Feĭnberg and D. S. Chernavskiĭ, Usp. Fiz. Nauk **82**, 3 (1964) [Sov. Phys. Usp. **7**, 1 (1964)].
[54]A. Ballestrero, E. Predazzi, and R. Page, Nuovo Cimento **A25**, 419 (1975). B. Carazza and A. Gandolfi, Lett. Nuovo Cimento **16**, 102 (1976).
[55]M. S. Marinov, Usp. Fiz. Nauk **121**, 377 (1976).
[56]E. L. Feĭnberg, Preprint No. 172, Physics Inst., USSR Academy of Sciences, Moscow, 1976.
[57]O. V. Kancheli, Pis'ma Zh. Eksp. Teor. Fiz. **11**, 397 (1970) [JETP Lett. **11**, 267 (1970)]. A. Mueller, Phys. Rev. **D2**, 224, 1963 (1970).
[58]V. N. Gribov, Zh. Eksp. Teor. Fiz. **53**, 654 (1967) [Sov. Phys. JETP **26**, 414 (1968)].
[59]V. N. Gribov and A. A. Migdal, Yad. Fiz. **8**, 1002, 1213 (1968) [Sov. J. Nucl. Phys. **8**, 583, 703 (1969)]; Zh. Eksp. Teor. Fiz. **55**, 1498 (1968) [Sov. Phys. JETP **28**, 784 (1969)].
[60]V. A. Abramovskiĭ, V. N. Gribov, and O. V. Kancheli, Yad. Fiz. **18**, 595 (1973) [Sov. J. Nucl. Phys. **18**, 308 (1974)].
[61]M. Ciafaloni and G. Marchesini, Nucl. Phys. **B105**, 113 (1976).
[62]I. V. Andreev, Yad. Fiz. **22**, 186 (1975) [Sov. J. Nucl. Phys. **22**, 92 (1975)].
[63]V. A. Abramovskiĭ, Pis'ma Zh. Eksp. Teor. Fiz. **23**, 228 (1976) [JETP Lett. **23**, 205 (1976)].
[64]A. Capella, J. Kaplan, and J. Tran-Thanh Van, Nucl. Phys. **B105**, 333 (1976).
[65]A. Capella and J. Kaplan, Phys. Lett. **B52**, 448 (1974). A. Capella, J. Tran-Thanh Van, and J. Kaplan, Nucl. Phys. **B97**, 493 (1975).
[66]H. Cheng, J. K. Walker, and T. T. Wu, Phys. Lett. **B44**, 97, 283 (1973).
[67]P. D. B. Collins, F. D. Gault, and A. Martin, Nucl. Phys. **B80**, 135 (1974). S. Y. Chu, B. R. Desai, B. C. Shen, and R. D. Feld, Phys. Rev. **D11**, 2967 (1976).
[68]C. Pajares and R. Pascual, *ibid.* **D14**, 258 (1976).
[69]M. S. Dubovikov, B. Z. Kopelevich, L. I. Lapidus, and K. A. Ter-Martirosyan, Preprint D2-9789, JINR, Dubna, 1976.
[70]A. Capella and A. Kaidalov, Preprint TH 2151, CERN, 1976.
[71]L. Caneschi, Nucl. Phys. **B88**, 77 (1974); **B108**, 417 (1976).
[72]H. D. I. Abarbanel, Rev. Mod. Phys. **48**, 435 (1976). H. D. I. Abarbanel, J. B. Bronzan, R. Sugar, and A. R. White, Phys. Rep. **21C**, 119 (1975).
[73]M. Ciafaloni, G. Marchesini, and G. Veneziano, Nucl. Phys. **B98**, 472, 493 (1975).
[74]A. A. Migdal, A. M. Polyakov, and A. K. Ter-Martirosyan, Phys. Lett. **B48**, 239 (1974); Zh. Eksp. Teor. Fiz. 67, 84 (1974) [Sov. Phys. JETP **40**, 43 (1975)].
[75]H. D. I. Abarbanel and J. B. Bronzan, Phys. Lett. **B48**, 345 (1974); Phys. Rev. **D9**, 2397 (1974).
[76]M. Baker, Nucl. Phys. **B80**, 61 (1974). J. Bronzan and J. Dash, Phys. Rev. **D10**, 4208 (1974).
[77]S. Dash and S. J. Harrington, Phys. Lett. **B57**, 78; **B59**, 249 (1975).
[78]J. Ellis and R. Swit, Nucl. Phys. **B94**, 477 (1975).
[79]H. D. I. Abarbanel, J. Bartels, J. B. Bronzan, and D. Sidhu, Phys. Rev. **D12**, 2459, 2798 (1975).
[80]W. R. Frazer and M. Moshe, *ibid.* **D12**, 2370, 2385 (1975).
[81]D. Amati and R. Jengo, Phys. Lett. **B56**, 465 (1975).
[82]H. D. I. Abarbanel, J. B. Bronzan, A. Schwimmer, and R. L. Sugar, Phys. Rev. **D14**, 632 (1976).
[83]A. R. White, Preprint TH 1237, CERN, 1976.
[84]A. Schwimmer, Nucl. Phys. **B94**, 445 (1975).
[85]D. Amati, L. Caneschi, and R. Jengo, *ibid.* **B101**, 397 (1975).
[86]M. Ciafaloni and G. Marchesini, *ibid.* **B109**, 261 (1976).
[87]J. L. Cardy, *ibid.* **B75**, 413 (1974).
[88]K. A. Ter-Martirosyan, Phys. Lett. **B44**, 377 (1973).
[89]D. R. Snyder and M. W. Wyld, Jr., Phys. Rev. **D11**, 2538 (1975).
[90]Yu. M. Shabel'skiĭ, Preprint LIYaF-114, Leningrad, 1975.
[91]E. M. Levin and M. G. Ryskin, Yad. Fiz. **21**, 366 (1975) [Sov. J. Nucl. Phys. **21**, 192 (1975)].
[92]W. Ko, J. Erwin, R. L. Lander, *et al.*, Phys. Lett. **B33**, 1443 (1974). R. Singer, Y. Cho, T. Fields, *et al.*, *ibid.* **B49**, 481 (1974).
[93]I. I. Roĭzen, Preprint No. 39, Physics Inst., USSR Academy of Sciences, Moscow, 1976; Yad. Fiz., to be published (1977).

[94]A. N, Sisakyan, Preprint E2-8825, JINR, Dubna, 1975.
[95]I. F. Ginzburg, L. I. Perlovskiĭ, and A. M. Vasylev, cited in Ref. 23a, p. 23.
[96]E. M. Levin and M. G. Ryskin, Yad. Fiz. **17**, 386 (1973) [Sov. J. Nucl. Phys. **17**, 196 (1973)]; **18**, 431 (1973) [**18**, 223 (1974)].
[97]E. L. Berger, Phys. Rev. Lett. **20**, 964; **21**, 701 (1968).
[98]K. G. Boreskov, A. B. Kaĭdalov, L. A. Ponomarev *et al.*, Yad. Fiz. **15**, 361, 557 (1972) [Sov. J. Nucl. Phys. **15**, 203, 309 (1972)]; **17**, 1285 (1973) [**17**, 669 (1973)].
[99]D. Griffiths, A. M. Saperstein, and D. T. Schnitzer, Phys. Rev. **D6**, 2546 (1972).
[100]I. M. Dremin, I. I. Roĭzen, R. B. White, and D. S. Chernavskiĭ, Zh. Eksp. Teor. Fiz. **48**, 952 (1965) [Sov. Phys. JETP **21**, 633 (1965)].
[101]E. I. Volkov, I. M. Dremin, T. I. Kanarek, and D. S. Chernavskiĭ, Preprint No. 40, Physics Inst., USSR Academy of Sciences, Moscow, 1976.
[102]S. Pokorski and L. Van Hove, Acta Phys. Pol. **B5**, 229 (1974).
[103]F. Hayot, F. Henyey, and M. Le Bellac, Nucl. Phys. **B80**, 77 (1974).
[104]G. Ranft and J. Ranft, Lett. Nuovo Cimento 10, 485 (1974); Nucl. Phys. **B83**, 285 (1975).
[105]J. Meunier and G. Plaut, *ibid.* **B87**, 74 (1975).
[106]R. P. Feynman, Photon-Hadron Interactions, Benjamin, Reading, Mass., 1972. J. D. Bjorken and E. A. Paschos, Phys. Rev. **185**, 1975 (1969); **D1**, 3151 (1970).
[107]E. M. Levin and L. L. Frankfurt, Pis'ma Zh. Eksp. Teor. Fiz. **3**, 652 (1965). H. J. Lipkin and F. Scherk, Phys. Rev. Lett. **16**, 71 (1966).
[108]H. Satz, Phys. Lett. **B25**, 220 (1967).
[109]I. N. Erofeeva *et al.*, Izv. Akad. Nauk SSSR Ser. Fiz. **31**, 1412 (1967). V. S. Murzin and L. I. Sarycheva, *ibid.* **34**, 1898 (1970).
[110]G. Eilam and Y. Gell, Phys. Rev. D10, 3634 (1974).
[111]S. P. K. Tavernier, Nucl. Phys. **B105**, 241 (1976). M. Deutchmann, in: Proc. of the Intern. Conf. on Elementary Particles (Amsterdam, 1971), North-Holland, Amsterdam, 1972.
[112]V. V. Anisovich and V. M. Shekhter, Nucl. Phys. **B55**, 433 (1973). V. V. Anisovich and M. N. Kobrinsky, Phys. Lett. **B46**, 419 (1973).
[113]V. N. Guman and V. M. Shekhter, Nucl. Phys. **B99**, 523 (1975); Preprint No. 216, LNPI, 1976.
[114]V. N. Guman and V. M. Shekhter, Yad. Fiz. **22**, 1237 (1975) [Sov. J. Nucl. Phys. 22, 642 (1975)].
[115]V. V. Anisovich, M. N. Kobrinskiĭ, and V. N. Povzun, cited in Ref. 23a, p. 23.
[116]A. K. Likhoded, V. A. Petrov, and A. N. Tolstenkov, Preprint OTF 76-2, IHEP, Serpukhov, 1976.
[117]L. Van Hove and S. Pokorski, Nucl. Phys. **B86**, 287 (1975).
[118]L. Van Hove and K. Fialkowski, Preprint TH 2123, CERN, 1976.
[119]V. Cerny, P. Lichard, and J. Pisut, cited in Ref. 23a, p. 23.
[120]H. Satz, *ibid.*, p. 23.
[121]E. I. Volkov, I. M. Dremin, A. M. Dunaevskiĭ, I. I. Roĭzen and D. S. Chernavskiĭ, Yad. Fiz. **20**, 149 (1974) [Sov. J. Nucl. Phys. **20**, 78 (1975)].
[122]D. S. Chernavskii, T. I. Kanarek, and E. I. Volkov, Preprint No. 54, P. N. Lebedev Inst., Moscow, 1975.
[123]E. I. Volkov and T. I. Kanarek, Preprint No. 115, Physics Inst., USSR Academy of Sciences, Moscow, 1975.
[124]I. V. Andreev, Yad. Fiz. **14**, 837 (1971) [Sov. J. Nucl. Phys. **14**, 468 (1972)]; Pis'ma Zh. Eksp. Teor. Fiz. **20**, 199 (1974) [JETP Lett. **20**, 85 (1974)].
[125]T. K. Gaisser and C. I. Tan, Phys. Rev. D8, 3881 (1973). M. Suzuki, Nucl. Phys. **B64**, 486 (1973). C. B. Chiu and D. M. Tow, Preprint ORO-263, 1976. S. T. Jones, Phys. Rev. D11, 692 (1975).
[126]L. É. Gendenshteĭn, A. B. Kaĭdalov, and D. S. Chernavskiĭ, Pis'ma Zh. Eksp. Teor. Fiz. **19**, 61 (1974) [JETP Lett. **19**, 38 (1974)].
[127]M. Chaichian, R. Hagedorn, and M. Hayashi, Nucl. Phys. **B92**, 445 (1975).
[128]D. Sivers, S. J. Brodsky, and R. Blankenbecler, Phys. Rep. **23C**, 1 (1976).
[129]E. L. Feĭnberg, Izv. Akad. Nauk SSSR Ser. Fiz. **26**, 622 (1962); **34**, 1987 (1970); Preprint TH2156-CERN, 1976.
[130]T. C. Meng, Phys. Rev. **D9**, 3062 (1974). K. W. Lai and T. C. Meng, Phys. Rev. Lett. **37**, 241 (1976).
[131]I. M. Dremin, Yad. Fiz. 18, 617 (1973) [Sov. J. Nucl. Phys. **18**, 362 (1973)].
[132]P. V. Landshoff, Preprint TH2227-CERN, 1976.
[133]F. C. Winkelmann *et al.*, Phys. Lett. **B56**, 101 (1976).
[134]D. Fong *et al.*, *ibid.* **B60**, 124 (1975).
[135]V. V. Ammosov *et al.*, Preprint M-19, IHEP, Serpukhov, 1975.
[136]N. Angelov and V. G. Grishin, cited in Ref. 23a, p. 14.
[137]P. V. Shlyapnikov, *ibid.*, A2-42.
[138]L. Foa, Phys. Rep. **22C**, 1 (1975) A. Gula, Lett. Nuovo Cimento **13**, 432 (1975). T. T. Gien, *ibid.*, p. 193.
[139]P. Darriulat, Invited talk at the 6th Intern. Colloquium on Multiparticle Reactions, Oxford, 1975. S. R. Amendolia, G. Bellettini, *et al.*, Nuovo Cimento **A31**, 17 (1976).
[140]E. L. Berger, Nucl. Phys. **B85**, 61 (1975).
[141]F. Hayot and M. Le Bellac, Nucl. Phys. **B86**, 333 (1975).
[142]C. B. Chiu and K.-H. Wang, Phys. Rev. **D13**, 3045 (1976). N. Murai, Phys. Lett. **B56**, 351 (1975).
[143]A. M. Gershkovich and I. M. Dremin, Kratk. Soobshch. Fiz., No. 1, 7 (1976).
[144]T. Ludlam and R. Slansky, Phys. Rev. **D12**, 59, 65 (1975).
[145]R. Baier and F. W. Bopp, *ibid.* D13, 2148 (1976).
[146]J. Iwai, N. Suzuki, and Y. Takahashi, Prog. Theor. Phys. **55**, 1537 (1976).
[147]T. Kafka *et al.*, Phys. Rev. Lett. **34**, 687 (1975). C. Bromberg *et al.*, Phys. Rev. **D9**, 1864 (1974); D12, 1224 (1975). J. W. Lamsa *et al.*, Phys. Rev. Lett. **37**, 73 (1976). Y. Hommo *et al.*, Lett. Nuovo Cimento **15**, 235 (1976).
[148]J. Benecke, in: Proc. of the 1972 Zakopane Colloquium, p. 429. T. T. Chou and C. N. Yang, Phys. Rev. **D7**, 1425 (1973). C. Quigg and G. H. Thomas, *ibid.*, p. 2752. A. Krzywicki and D. Weingarten, Phys. Lett. **B50**, 265 (1974). A. Bialas, Preprint, Jagellonian University, 1974. R. Baier and F. Bopp, Preprint Bi-74/06, 1974. C. B. Chiu and K.-H. Wang, Preprint ORO-3992-231, 1976.
[149]I. Ya. Pomeranchuk and E. L. Feĭnberg, Dokl. Akad. Nauk SSSR **95**, 439 (1953).
[150]E. L. Feĭnberg, Zh. Eksp. Teor. Fiz. **50**, 202 (1966) [Sov. Phys. JETP **23**, 132 (1966)]; Lectures at the Sukhumi School for Young Scientists, Preprint No. 166, Physics Inst., USSR Academy of Sciences, Moscow, 1972.
[151]V. N. Gribov, 1st ITEP School of Physics, No. 1, 1973, p. 65. A. A. Ansel'm, *ibid.*, No. 2, p. 3.
[152]I. L. Rozental' and D. S. Chernavskiĭ, Usp. Fiz. Nauk **52**, 185 (1954).
[153]S. Z. Belen'kiĭ and A. D. Landau, Usp. Fiz. Nauk **56**, 309 (1955). S. Z. Belen'kiĭ and G. A. Milekhin, Zh. Eksp. Teor. Fiz. **29**, 920 (1955). G. A. Milekhin, Tr. Fiz. Inst. Akad. Nauk SSSR 16, 51 (1961).
[154]A. A. Emel'yanov, *ibid.* **29**, 169 (1965).
[155]É. V. Shuryak, cited in Ref. 23a, p. 23.
[156]O. V. Kancheli, Pis'ma Zh. Eksp. Teor. Fiz. **18**, 465 (1973) [JETP Lett. 18, 274 (1973)].
[157]A. Schwimmer, Nucl. Phys. B94, 445 (1975).
[158]J. Koplik and A. H. Mueller, Phys. Rev. **D12**, 3638 (1975).
[159]N. N. Nikolaev, Preprint ITF-18, 1975; ITF-930, 1976 (Chernogolovka). G. V. Davidenko and N. N. Nikolaev, Yad. Fiz. **24**, 772 (1976) [Sov. J. Nucl. Phys. **24**, 402 (1976)].
[160]R. J. Glauber, in: Lectures in Theoretical Physics, Vol. 1, Interscience, New York, 1959, p. 315.

[161]V. N. Gribov, Zh. Eksp. Teor. Fiz. **56**, 892 (1969) [Sov. Phys. JETP **29**, 483 (1969)]; **57**, 1306 (1969) [**30**, 709 (1970)].
[162]L. Bertocchi, Nuovo Cimento **11**, 45 (1972).
[163]J. H. Weis, Preprint TH-2197, CERN, 1976.
[164]I. V. Andreev and V. Kh. Khoruzhiĭ, Yad. Fiz. **12**, 191 (1970) [Sov. J. Nucl. Phys. **12**, 102 (1971)]. I. V. Andreev, Preprint No. 103, Physics Inst., USSR Academy of Sciences, Moscow, 1972.
[165]I. V. Andreev, Yad. Fiz. **22**, 186 (1975) [Sov. J. Nucl. Phys. **22**, 92 (1975)].
[166]L. Bertocchi and D. Treleani, Preprint TH-2215, CERN, 1976.
[167]Yu. M. Shabel'skiĭ, Preprint No. 248, Leningrad Inst. of Nuclear Physics, 1976.
[168]B. N. Kalinkin and V. L. Shmonin, Yad. Fiz. **21**, 628 (1975) [Sov. J. Nucl. Phys. **21**, 325 (1975)].
[169]K. Gottfried, Phys. Rev. Lett. **32**, 957 (1974).
[170]A. Dar and J. Vary, Phys. Rev. **D6**, 2412 (1972).
[171]G. Berlad, A. Dar, and G. Eilam, *ibid.* **D13**, 161 (1976).
[172]A. Z. Patashinskiĭ, Pis'ma Zh. Eksp. Teor. Fiz. **19**, 654 (1974) [JETP Lett. **19**, 338 (1974)].
[173]P. M. Fishbane and J. S. Trefil, Phys. Lett. **51B**, 179 (1974).
[174]A. Bialas and E. Bialas, Acta Phys. Pol. **B5**, 373 (1974).
[175]I. V. Andreev and I. M. Dremin, Yad. Fiz. **9**, 176 (1969) [Sov. J. Nucl. Phys. **9**, 106 (1969)].
[176]V. N. Gribov, B. L. Ioffe, and I. Ya. Pomeranchuk, Yad. Fiz. **2**, 768 (1965) [Sov. J. Nucl. Phys. **2**, 549 (1966)].
[177]B. L. Ioffe, Phys. Lett. **B30**, 123 (1969).
[178]I. V. Andreev, Preprint No. 59, Physics Inst., USSR Academy of Sciences, Moscow, 1975.
[179]O. V. Kancheli, Pis'ma Zh. Eksp. Teor. Fiz. **22**, 491 (1975) [JETP Lett. **22**, 237 (1975)]; cited in Ref. 23a, p. 23.
[180]L. D. Landau and I. Ya. Pomeranchuk, Dokl. Akad. Nauk SSSR **92**, 535, 735 (1953).
[181]M. L. Ter-Mikaelyan, Zh. Eksp. Teor. Fiz. **25**, 289, 296 (1953).
[182]E. L. Feĭnberg, Zh. Eksp. Teor. Fiz. **28**, 242 (1955) [Sov. Phys. JETP **1**, 177 (1955)]; **29**, 115 (1955) [**2**, 58 (1956)].
[183]G. T. Zatsepin, Izv. Akad. Nauk SSSR Ser. Fiz. **26**, 674 (1962).
[184]C. Bemporad *et al.*, Nucl. Phys. **B33**, 397 (1971); **B42**, 627 (1972). W. Beusch, Acta Phys. Pol. **B3**, 679 (1972).
[185]V. S. Murzin and L. I. Sarycheva, Yad. Fiz. **23**, 383 (1976) [Sov. J. Nucl. Phys. **23**, 199 (1976)]. A. I. Demianov *et al.*, in: Proc. of the 14th Intern. Conf. on Cosmic Rays, Vol. 7, Munich, 1975, p. 2522. A. I. Dem'yanov, V. S. Murzin, and L. I. Sarycheva, cited in Ref. 23a, p. 27.
[186]J. Pumplin, Phys. Rev. **D8**, 2899 (1973).
[187]N. Sakai and J. N. J. White, Nucl. Phys. **B59**, 511 (1973).
[188]H. I. Miettinen, Preprint TH 1864, CERN, 1974.
[189]L. Caneschi, P. Grassberger, H. I. Miettinen, and F. Henyey, Phys. Lett. **B56**, 359 (1975).
[190]B. R. Webber, *ibid.* **B49**, 474 (1974).
[191]P. Bosetti *et al.*, Nucl. Phys. **B97**, 29 (1975).
[192]B. R. Webber *et al.*, *ibid.*, p. 317.
[193]F. S. Henyey and J. Pumplin, cited in Ref. 23a, p. 23.
[194]G. Goldhaber, S. Goldhaber, *et al.*, Phys. Rev. **120**, 300 (1960).
[195]G. I. Kopylov and M. I. Podgoretskiĭ, Yad. Fiz. **14**, 1081 (1971) [Sov. J. Nucl. Phys. **14**, 604 (1972)]; **15**, 392 (1972) [**15**, 219 (1972)]; 18, 656 (1973) [**18**, 336 (1974)]; **19**, 434 (1974) [19, 215 (1974)]; cited in Ref. 23a, p. 11.
[196]G. J. Kopylov, Phys. Lett. **B50**, 472 (1974).
[197]E. V. Shuryak, *ibid.* **B44**, 387 (1973).
[198]G. Cocconi, *ibid.* **B49**, 459 (1974).
[199]R. Hanbury Brown and R. Q. Twiss, Philos. Mag. **45**, 663 (1964).
[200]G. S. Gorelik, Dokl. Akad. Nauk SSSR **58**, 45 (1947); Usp. Fiz. Nauk **34**, 321 (1948).
[201]M. Deutschmann *et al.*, Nucl. Phys. B103, 198 (1976).
[202]E. Calligarich *et al.*, Lett. Nuovo Cimento **16**, 129 (1976).
[203]F. Grard *et al.*, Nucl. Phys. B102, 221 (1976).
[204]V. G. Grishin, Preprint D12-9224, JINR, Dubna, 1975.
[205]A. M. Dunaevskiĭ, A. V. Uryson, *et al.*, cited in Ref. 23a, p. 11.
[206]V. S. Aseĭkin, V. P. Bobova, *et al.*, Izv. Akad. Nauk SSSR Ser. Fiz. **38**, 998 (1974).
[207]S. I. Nikolsky, V. P. Pavluchenko, E. L. Feinberg, and V. I. Yakovlev, Preprint No. 69, P. N. Lebedev Inst., Moscow, 1975.
[208]V. P. Pavlyuchenko, S. I. Nikol'skiĭ, and V. I. Yakovlev, cited in Ref. 23a, p. 11.
[209]S. I. Nikol'skiĭ and V. I. Yakovlev, Kratk. Soobshch. Fiz., No. 5, 13 (1976).
[210]Japanese-Brasilian Collaboration, CKJ Report-13, 1974; Proc. of the 14th Intern. Conf. on Cosmic Rays, Munich, 1975.
[211]M. Miesowicz, in: Progress in Elementary Particles and Cosmic Ray Physics, Vol. 10, ed. J. G. Wilson and S. A. Wouthuysen, North-Holland, Amsterdam, 1971, p. 103.

Translated by N. M. Queen